

1 **Response of active catchment water storage capacity**  
2 **to the prolonged meteorological drought and**  
3 **asymptotic climate variation**

4

5 **Jing Tian<sup>1</sup>, Zhengke Pan<sup>1,2</sup>, Shenglian Guo<sup>1\*</sup>, Jiabo Yin<sup>1</sup>, Yanlai Zhou<sup>1</sup>, Jun Wang<sup>1</sup>**

6

7 <sup>1</sup>State Key Laboratory of Water Resources and Hydropower Engineering Science,

8 Wuhan University, Wuhan 430072, China

9

10 <sup>2</sup>Changjiang Institute of Survey, Planning, Design and Research, Wuhan, 430010,

11 China

12

13 \*Corresponding author. Email: [slguo@whu.edu.cn](mailto:slguo@whu.edu.cn)

14 **Abstract:** Studies on the hydrological response to continuous extreme and asymptotic  
15 climate change can improve our ability to cope with the intensified water-related  
16 problems. Most of the literature focused on the runoff response to climate change, while  
17 neglecting the impacts of the potential variation in the active catchment water storage  
18 capacity (ACWSC) that plays an essential role in the transfer of climate input to the  
19 catchment runoff. This study aims to systematically identify the response of the  
20 ACWSC to the long-term meteorological drought and asymptotic climate change.  
21 Firstly, the time-varying parameter is derived to reflect the ACWSC periodic/abrupt  
22 variations in both drought and non-drought periods. Secondly, the change points and  
23 varying patterns of the ACWSC are analyzed based on the Bayesian change point  
24 analysis with multiple evaluation criteria. Finally, various catchment properties and  
25 climate characteristics are used to explore the possible relationship between these  
26 variables and the temporal variation characteristics of the ACWSC. The catchments that  
27 suffered from the prolonged meteorological drought in southeast Australia were  
28 selected as the case study. Results indicate that: (1) the increase of amplitude change in  
29 the ACWSC is observed in 83/92 catchments during the prolonged drought period, and  
30 significant shifts in the mean value of the ACWSC are detected in 77/92 catchments;  
31 (2) the average response time of the ACWSC for all 92 catchments with significant  
32 changes is 641.3 days; (3) the values of the ACWSC are changed significantly in the  
33 catchments with small areas, low elevations, small slope ranges, large forest coverage,  
34 and high soil water holding capacities. This study could enhance our understanding of

35 the variations in catchment property under climate change.

36 **Keywords:** catchment water storage capacity; prolonged meteorological drought;

37 extreme and asymptotic climate change; southeast Australia

## 38 **1. Introduction**

39 Climate change has been one of the most important drivers influencing the mechanism  
40 of runoff generation and the confluence process of catchments (Jung et al.,  
41 2012; Changnon and Gensini, 2019). Depending on the extent and duration of climate  
42 change, it could be classified into extreme (e.g., from prolonged meteorological drought  
43 to extremely wet conditions in a period) and asymptotic changes (climate change in  
44 different seasons in a normal year). For instance, significant variations (i.e., less runoff  
45 than expected) in hydrological behavior have been reported during the decade-long  
46 millennium drought of many catchments in south-eastern Australia compared with the  
47 previous wet period (Saft et al., 2016). In addition, seasonally asymptotic variations  
48 have been identified in many catchments in America due to the seasonal growth and  
49 die-off of vegetation (Deng et al., 2018; Pan et al., 2019a), Asia (Deng et al., 2016) and  
50 Australia (Pan et al., 2019b). Studies on the hydrological response of catchments to  
51 different climate change scenarios not only can improve our understanding of the  
52 hydrological variation mechanism of the catchment, but also enhance our ability to  
53 prevent unpredictable extreme events.(Kusangaya et al., 2014; Kundu et al., 2017).

54 Accordingly, studies on the hydrological response to the changing environments  
55 generally included two main approaches, i.e., statistical analysis and hydrological

56 modeling. Statistical analysis methods can be used to detect trend changes of prolonged  
57 hydrological and meteorological data series (Costa et al., 2003; Siriwardena et al.,  
58 2006); nevertheless, they usually lack sufficient physical explanations for the potential  
59 variation in catchment hydrological response (Lin et al., 2015; Liu et al., 2018).  
60 Hydrological models that can comprehensively consider the spatial heterogeneity and  
61 physical process of the catchment are broadly used to quantify the hydrological  
62 response under multiple climate conditions (Abbaspour et al., 2007; Tu, 2009; Chen et  
63 al., 2019; Tian et al., 2021). For example, Chawla and Mujumdar (2015) adopted the  
64 Variable Infiltration Capacity (VIC) model to evaluate the runoff response in the upper  
65 Ganga basin. Shen et al. (2018) adopted the Hydrological Model of École de  
66 Technologies Supérieure (HMETS) to estimate the uncertainty of runoff response to  
67 climate change. Tian et al. (2021) applied the Soil and Water Assessment Tool (SWAT)  
68 model to assess the effects of climate change on future runoff in the Han River basin,  
69 China. However, most of the previous studies on hydrologic response mainly focused  
70 on the variations in runoff response to climate change, without paying attention to the  
71 causality between the varying climates (i.e., extreme, and asymptotic changes of  
72 climates) and variation in catchment properties.

73 Many previous studies (McNamara et al., 2011; Melsen et al., 2016; Carrer et al.,  
74 2019) indicated that the catchment water storage capacity (ACWSC) is one of the most  
75 significant parameters influencing the mechanism of hydrological response of  
76 catchments. The ACWSC is defined as ‘the active water storage capacity refers to the

77 maximum volume of water stored within a catchment and its distribution among  
78 groundwater, soil moisture, vegetation, surface water, and snowpack, which are the  
79 variables that ultimately characterize the state of the hydrological system' (McNamara  
80 et al., 2011). The root zone storage capacity is defined as "the maximum amount of soil  
81 moisture that can be accessed by vegetation for transpiration" (Gao et al., 2014; Nijzink  
82 et al., 2016; Singh et al., 2020; Laurène, 2021). For a given catchment, the value of the  
83 ACWSC should be greater than or equal to the root zone storage capacity.

84 Our previous study identified the impact of meteorological drought on the  
85 ACWSC by investigating the changes in hydrological model parameters before and  
86 after drought events (Pan et al., 2020). Results showed that significant shifts in the  
87 ACWSC were identified in almost two-thirds of the catchments in south-eastern  
88 Australia during the prolonged meteorological drought period. Two subsets of  
89 catchments with opposite response directions were identified in the study area, i.e., the  
90 subsets of catchments with reduced and increased runoff generation rates, respectively.  
91 The main potential reasons may be the difference in the proportion of evergreen  
92 broadleaf forests in these catchments. We only considered the average shifts from the  
93 non-drought period to the drought period and treated the ACWSC of each period as a  
94 constant while neglecting the time-varying characteristics of the ACWSC of each  
95 catchment due to the periodic climate change, and thus were unable to reflect variation  
96 in catchment characteristics under asymptotic climate.

97 Recently, studies of the potential time-varying ACWSC characteristics based on

98 the simulation of the temporal variations of hydrological parameters have attracted a  
99 lot of attention (Coron et al., 2012; Brigode et al., 2013; Patil and Stieglitz, 2015; Deng  
100 et al., 2018), and provided a new approach for better-representing changes in catchment  
101 characteristics (Deng et al., 2016). Accordingly, the selected model parameters that  
102 refer to the ACWSC in the model structure were constructed as multiple hypothetical  
103 functions based on physical covariates (e.g., time covariates and catchment attributes),  
104 and their simulation results were evaluated and compared with observations through  
105 specific criteria. Thus, the functional form that achieved the best simulation  
106 performance would be recognized as the best item to represent the potential changes in  
107 the catchment property (Jeremiah et al., 2013; Westra et al., 2014; Pan et al., 2019a;  
108 Pan et al., 2019b).

109 In this study, we systematically explore the response of the ACWSC to both  
110 extreme climate changes (i.e., prolonged meteorological drought) and asymptotically  
111 periodic climate changes. Three scientific questions will be investigated as follows.

112 (1) What are the change characteristics of the ACWSC under the conditions of  
113 prolonged meteorological drought and asymptotic climate variation?

114 (2) Which catchment features and climate factors are more likely to relate to the  
115 change of the ACWSC?

116 (3) What is the difference in the ACWSC when both extreme climate variation and  
117 asymptotic climate variation are considered compared with extreme climate variation?

## 118 **2. Materials**

### 119 **2.1. Study area**

120 In this study, south-eastern Australia was selected as the initial study area. To minimize  
121 the impact of human activities, 398 catchments that were not disturbed by reservoirs or  
122 irrigation systems are selected in this study. The study area extends from southern  
123 Victoria to New South Wales and Queensland. The study area and the locations of the  
124 398 initial catchments are illustrated in **Fig. 1**. Saft et al. (2015) and Pan et al. (2019b)  
125 indicated that these catchments had experienced about ten years of meteorological  
126 drought near the millennium, which had a significant impact on the stability of local  
127 ecosystems and the development of society, economy, and politics (Nicholls, 2004; Hunt,  
128 2009; Potter et al., 2011; Hughes et al., 2012; van Dijk et al., 2013; Saft et al., 2015).

129 The essential climate characteristics include the large proportion of arid areas, the  
130 semi-annular distribution of annual precipitation, and the terrain, geology, land cover,  
131 and climate conditions are differentiated between various state catchments. The annual  
132 mean precipitation and temperature range from 507 mm to 1814 mm and 8.26°C to  
133 19.52°C, respectively. From the perspective of spatial and temporal distribution, the  
134 precipitation in the catchments of Victoria state is mainly concentrated in winter. In  
135 contrast, the northern catchments in New South Wales and Queensland states have more  
136 rain in summer than in winter. The potential reason for this phenomenon is ENSO (El  
137 Niño-Southern Oscillation). In terms of runoff, runoff in summer is dominant in

138 northern catchments, while runoff in winter is more likely to occur in southern  
139 catchments.

## 140 **2.2. Data set**

141 **Table 1** summarized the description and source of the three types of data sets, which  
142 include (1) meteorological data (daily precipitation and potential evapotranspiration  
143 (PET)), (2) hydrological data (daily runoff), and (3) catchment characteristics  
144 (catchment area, mean elevation, mean slope, forest coverage percentage, etc.).

145 398 catchments were selected by Zhang et al. (2013), with catchment areas ranging  
146 from 50 km<sup>2</sup> to 17000 km<sup>2</sup>. The collection period of observations of these catchments  
147 ranges from 1976 to 2011. It is noted that the historical meteorological observations of  
148 all catchments in the data sets were complete. However, the daily runoff observations  
149 of 125 catchments were incomplete with the integrity of the time series being less than  
150 80%. Thus, these catchments were excluded, and the remaining 273 catchments were  
151 used for meteorological drought identification. Finally, 145 catchments were identified  
152 through a long-term meteorological drought with a drought period longer than seven  
153 years. The drought periods corresponding to those 145 catchments are exhibited in  
154 **Fig.2**. Based on the identification criteria of the prolonged drought period, all the  
155 drought periods in these catchments lasted more than seven years. In addition, the  
156 drought periods of 35% of the catchments spanned over thirteen years. It can be found  
157 that the prolonged meteorological drought of most catchments started after 1990 and



158 ended before 2009. In particular, the meteorological drought of 34 catchments began in  
159 1997, and 37 catchments began in 2001.

160 The characteristics of the 145 catchments with prolonged meteorological drought  
161 (**Table 2**) demonstrate that there are significant differences in physical properties  
162 among different catchments. For example, the catchment area, mean elevation, and  
163 mean slope range from 54 to 6818 km<sup>2</sup>, from 47 to 1351m, and from 0.3 to 13.6°,  
164 respectively. The interval of forest coverage is [15%, 92%]. These catchment features  
165 were selected as potential impact factors and analyzed further in Section 4.3.

### 166 **3. Methodology**

167 The proposed methodology and procedures are sketched in **Fig.3**. To investigate the  
168 response of the ACWSC to the prolonged meteorological drought and asymptotic  
169 climate variation, the study scheme is conducted with the following four procedures:  
170 (1) identification of prolonged meteorological drought; (2) derivation of the response  
171 of the ACWSC to long-term meteorological drought and asymptotic climate variation  
172 based on the Bayesian change point analysis and the hydrological modeling approach;  
173 and (3) analysis of potential factors (i.e., properties of the catchments and climate  
174 characteristics) that may be related to the potential changes of the ACWSC and the  
175 response time (defined as the time interval between the occurrence of the prolonged  
176 meteorological drought and the abrupt shift of the ACWSC).

### 177 **3.1. Identification of prolonged meteorological drought**

178 There are many methods/indexes, such as the Standardized Precipitation Index (SPI)  
179 (Bayat et al., 2015), Rainfall Departure Analysis (Kumar et al., 2020), and Standardized  
180 Precipitation-Evapotranspiration Index (SPEI) (Das et al., 2021), have been used to  
181 identify the prolonged meteorological drought. Saft et al. (2015) introduced a drought  
182 definition algorithm that was based on the annual rainfall only and proved to have a  
183 lower degree of dependence and more robustness than other selected approaches in the  
184 south-eastern Australia catchments. It is mentioned that the prolonged drought period  
185 should be longer than 7 years according to the defined algorithm. For more detailed  
186 information about this method, please refer to Saft et al. (2015) and Pan et al. (2019b).

### 187 **3.2. Hydrological model**

188 The GR4J hydrological model (modèle du Génie Rural à 4 paramètres Journalier) was  
189 used to simulate the potential change characteristics of the ACWSC before and after  
190 the prolonged meteorological drought. The GR4J model is a daily lumped rainfall-  
191 runoff model developed by Perrin et al. (2003) and improved by Le Moine et al. (2008),  
192 and it has been used in more than 400 regions with various climatic characteristics  
193 around the world, such as China (Zeng et al., 2019), France (Perrin et al., 2003), North  
194 America (Pan et al., 2019a), and Australia (Coron et al., 2012). Its validity in the  
195 simulation of the rainfall-runoff relationship and reflection of potential changes in  
196 catchment properties has been verified by Le Moine et al. (2008) and Simonneaux et al.

197 (2008).

### 198 **3.2.1 Model structure**

199 The original GR4J model framework proposed by Perrin et al. (2003) only contains  
200 four parameters, and its structure is shown in **Fig.4**. The meanings of the four model  
201 parameters are introduced as follows:  $\theta_1$  is the maximum capacity of the soil moisture  
202 accounting storage, which is used to represent the ACWSC (mm) in this study;  $\theta_2$  is the  
203 groundwater exchange coefficient (mm);  $\theta_3$  represents the one-day-ahead maximum  
204 capacity of the routing storage (mm); and  $\theta_4$  is the time base of unit hydrograph UH1  
205 (day). All model parameters are real values,  $\theta_1$ ,  $\theta_3$  and  $\theta_4$  are positive, and  $\theta_2$  can be  
206 positive, negative, or 0.

207 Based on the existing data and catchment attributes, it is almost impossible to  
208 obtain the real value of the ACWSC with current technology. However, the hydrological  
209 simulation method provides a new perspective for revealing the potential changes of  
210 the ACWSC, i.e., we can use a specific parameter ( $\theta_1$ ) in the GR4J model to represent  
211 the ACWSC and characterize its variation in the real catchment. Similar studies can be  
212 found in Westra et al. (2014), and Deng et al. (2016). Hence, the simulated values of  
213 parameter  $\theta_1$  and its time-varying characteristics are used to represent the change of the  
214 real ACWSC. It should be noted that  $\theta_2$ ,  $\theta_3$  and  $\theta_4$  are assumed to remain constant;  
215 similar parameter settings can be found in previous studies (Westra et al., 2014; Pan et  
216 al., 2020).

### 217 **3.2.2 Periodicity of the ACWSC**

218 As explained, parameter  $\theta_l$  in the GR4J model was used to represent the real ACWSC  
219 according to its implications. Our previous work (Pan et al., 2020) verified that the  
220 ACWSC (i.e., parameter  $\theta_l$ ) had an “abrupt” point after the prolonged meteorological  
221 drought, which assumes that the offset of the estimated  $\theta_l$  represents the change of the  
222 ACWSC. Meanwhile,  $\theta_l$  in each period is recognized as a constant value and does not  
223 include the periodicity of the ACWSC that were outlined by many previous works  
224 (Nepal et al., 2017; Kunnath-Poovakka and Eldho, 2019; Sezen and Partal, 2019).  
225 However, Westra et al. (2014) and Pan et al. (2020) indicated that the ACWSC had  
226 periodic variability that may be due to the seasonal growth and wiling of catchment  
227 vegetation.

228 In this study, the potentially periodic variation characteristics of the ACWSC  
229 (represented by GR4J model parameter  $\theta_l$ ) were included to reflect the asymptotic  
230 change within different periods (i.e., periods before and after the change-point), which  
231 was described by the sine function. The sine function is one of the most fundamental  
232 functional forms to represent the periodic change of variables (Westra et al., 2014; Pan  
233 et al., 2019a; Pan et al., 2019b). Furthermore, the potentially extreme change of the  
234 ACWSC between the two periods was denoted by the variations between Equations (1)  
235 and (2). The time-varying functions of  $\theta_l$  during two periods are presented as follows:

236 Before the change-point:

$$\theta_1 = \alpha_1 \sin(\beta_1 t + \gamma_1) + \delta_1 \quad (1)$$

237 After the change-point:

$$\theta_1' = \alpha_2 \sin(\beta_2 t + \gamma_2) + \delta_2 \quad (2)$$

238 where,  $\alpha_1, \beta_1, \gamma_1, \delta_1$  and  $\alpha_2, \beta_2, \gamma_2, \delta_2$  are regression parameters for the time-varying  
 239 function;  $\alpha_1$  and  $\alpha_2$  signify the amplitude of the sine function;  $\beta_1$  and  $\beta_2$  represent  
 240 the frequency of the sine function;  $\gamma_1$  and  $\gamma_2$  denotes the remainder in the sine function;  
 241  $\delta_1$  and  $\delta_2$  refer to the intercept.

### 242 3.2.3 Likelihood function and parameter estimation

#### 243 (1) Likelihood function

244 In this study, the likelihood function for catchment  $i$  from Thiemann et al. (2001)  
 245 was adopted, which is shown as follows.

$$p_i(\theta(i) / \xi(i), q(i), r) \propto \left[ \frac{w(r)}{\sigma} \right]^T \exp \left[ -i(r) \sum_{t=1}^T \left| \frac{e_t(\theta(i))}{\sigma} \right|^{2/(1+r)} \right] \cdot p(\theta(i)) \quad (3)$$

$$\omega(r) = \frac{\{\Gamma[3(1+r)/2]\}^{1/2}}{(1+r) \left\{ \Gamma[(1+r)/2] \right\}^{3/2}}, \beta(r) = \left\{ \frac{\Gamma[3(1+r)/2]}{\Gamma[(1+r)/2]} \right\}^{1/(1+r)} \quad (4)$$

246 where  $p$  means the probability of likelihood.  $\theta(i) = (\theta_1, \theta_2, \theta_3, \theta_4)$ ;  $\Gamma(\cdot)$  denotes the  
 247 gamma function;  $T$  is the number of time steps;  $q$  represents the measured runoff;  $\xi$   
 248 denotes the climate variable input into the hydrological model;  $e_t$  refers to the residual  
 249 error at time step  $t$ ; and  $r$  is the type of the residual-error model (in this study,  $r$  is  
 250 represented by Gaussian distribution). When verifying the model type of the residual,

251 parameters  $\omega(r), \beta(r)$  are constant values as  $r$  is certain. In addition, the prior  
252 distribution of all unknown quantities is the uniform distribution.

## 253 **(2) Parameter estimation**

254 The posterior distribution of all unknown variables was estimated using the  
255 Shuffled complex evolution metropolis (SCEM-UA) algorithm, which was based on  
256 the Markov chain Monte Carlo method (Vrugt et al., 2003; Ajami et al., 2007). For the  
257 convergence of parameters, the Gelman-Rubin convergence value was selected as the  
258 evaluation standard, and the convergence threshold was 1.2. The pre-set ranges of all  
259 parameters are shown in **Table 3**.

## 260 **3.3 Change point analysis of ACWSC**

### 261 **3.3.1 Bayesian change point analysis**

262 The Bayesian change point analysis is one of the strongest ways available to explore  
263 the possible change time of the ACWSC (Carlin et al., 1992; Cahill et al., 2015). The  
264 likelihood probability was used to evaluate the possibility of each potential change  
265 point. The most likely time point of each potential scheme is regarded as the ultimate  
266 change point of that catchment.

### 267 **3.3.2 Criteria for evaluating significant changes in ACWSC**

268 To evaluate whether the ACWSC changed significantly under climate change, the  
269 following three criteria were adopted.

270 **(1) The Nash-Sutcliffe efficiency coefficient**

271 To guarantee the reasonable simulation results of the GR4J model, the Nash-  
272 Sutcliffe efficiency (NSE) coefficient values before and after the change point should  
273 be greater than 0.6. Furthermore, the difference in NSE values between the two periods  
274 should be less than  $|\pm 20\%|$ .

275 **(2) The minimum requirements for significant changes in storage capacity**

276 The change rate of the estimated parameter  $\theta_l$  ( $\theta'_l$ ) before and after the change  
277 point should exceed  $|\pm 20\%|$ . i.e.,  $\left| \frac{\theta'_l - \theta_l}{\theta_l} \right| \times 100\% \geq 20\%$ .

278 **(3) Robustness requirements of the results**

279 The initial values of model parameters were created three times to reduce their  
280 impacts on the final simulation results. Moreover, only the catchments that have  
281 significant changes in computation results will be taken as the final change items. If the  
282 simulation results meet such robustness requirements, the results would have the lowest  
283 dependency and the strongest stability on the adopted algorithm and model.

284 **3.4. Response time of a catchment**

285 Van Lanen et al. (2013) and Huang et al. (2017) showed that the recharge between the  
286 groundwater and surface runoff would alleviate the hydrological response under short-  
287 term meteorological drought. In other words, groundwater would buffer the surface  
288 runoff during the drought period. If the duration of the meteorological drought was

289 longer than several years or even decades, the hydraulic connection between the surface  
290 runoff and the underground runoff would be weak due to the gradual decrease of  
291 groundwater level. For example, Pan et al. (2020) indicated that the ACWSC may  
292 change with the occurrence of the prolonged meteorological drought, and the potential  
293 reasons were the difference in soil composition and the extensive death of vegetation  
294 during the drought period. It also should be noted that the ACWSC would not change  
295 immediately after the occurrence of the meteorological drought but respond after a  
296 period due to the existence of catchment elasticity (e.g., the existence of the hydraulic  
297 connection between surface runoff and groundwater). Thus, the time interval between  
298 the occurrence of the meteorological drought and the change point of the ACWSC is  
299 named the catchment response time.

### 300 **3.5 Potential factors associated with the changes in ACWSC**

301 The process that leads to the change of the ACWSC cannot be measured directly, so  
302 some measurable factors are used to probe the lurking correlation between the change  
303 of the ACWSC and the catchment response time. We select 33 potential factors of  
304 catchments and list them in **Table 4**, which includes 9 catchment features and 24 local  
305 climate variables. It is noted that because of the limitation of available data for  
306 catchment characteristics, only one static/constant value of the catchment features (A1-  
307 A9) was used for the correlation analysis. Furthermore, climate variables in four-time  
308 scales were used, including daily (B1-B4), monthly (B5-B7), seasonal (B8-B15), and  
309 annual (B16-B24) variables.



## 310 **4. Results**

### 311 **4.1 Change pattern of the ACWSC**

312 The most likely change point was confirmed when three criteria had been satisfied. The  
313 changing pattern of the ACWSC was determined by Equations (1) and (2). In other  
314 words, Equation (1)/Equation (2) reflects the potential periodic/asymptotic feature  
315 during the period before/after the change point. It is obvious that  $\alpha_1$  ( $\alpha_2$ ) and  $\delta_1$  ( $\delta_2$ )  
316 are the most important parameters in the regression function, which refer to the  
317 amplitude and intercept of the time-varying parameter  $\theta_1$ , respectively. Furthermore, the  
318 variation between  $\delta_1$  and  $\delta_2$  denotes the average difference between  $\theta_1$  and  $\theta_1'$ ,  
319 reflecting the potential change between the ACWSC of periods before and after the  
320 change point.

321 **Table 5** presents the variation characteristics (amplitude  $\alpha$  and mean value  $\delta$  of  
322 the ACWSC in the 145 studied catchments with meteorological drought in south-  
323 eastern Australia. The results showed that 36.6% of the catchments (55 of 145  
324 catchments) were identified to violate the criteria of the maximum performance  
325 degradation and result robustness, and thus were removed from further analysis. The  
326 remaining 92 catchments were retained as the-set of catchments that satisfied the basic  
327 criteria of NSE performance and resultant robustness. As presented in Equations (1)  
328 and (2), amplitude  $\alpha$  represents the range of variation in the ACWSC, a larger  $|\alpha|$   
329 implies a greater variation interval of the ACWSC during the specific period.  
330 Significant changes in amplitude  $\alpha$  were found in 60.0% of the catchments (87 of 145

331 catchments) during the drought period, in which 57.2% of the catchments (83 of 145  
332 catchments) experienced a significantly increased change in amplitude  $\alpha$  while 2.8%  
333 of the catchments (4 of 145 catchments) had significantly decreased variation during  
334 the drought period. In addition, only 3.4% of the catchments (5 of 145 catchments)  
335 experienced a non-significant change in amplitude  $\alpha$ , in which 3 (2) catchments had a  
336 slight increase (decrease) trend. It means that most of the catchments (87 of 92  
337 catchments) experienced a significant increase trend in the range of variation during the  
338 prolonged drought period (Table 5), indicating an increased dramatic cyclical variation  
339 magnitude of the ACWSC during the transformation from the non-drought period to  
340 the prolonged drought period.

341 The regression parameter  $\delta$ , which refers to the intercept/mean value of the  
342 ACWSC during the specific period, was used to evaluate the average difference  
343 between the ACWSC during the two periods. As Table 5 indicated: a significant  
344 increase in mean value  $\delta$  was identified in 84% of the catchments (77 of 145  
345 catchments) after the change point, but no catchment was found to experience a  
346 significant decrease of  $\delta$  during the drought period. In addition, the number of  
347 catchments with non-significant changes in  $\delta$  was 15, and 6.9% of the catchments (10  
348 of 145 catchments) and 3.5% of the catchments (5 of 145 catchments) were identified  
349 to have a non-significant increase and decrease trend during the drought period,  
350 respectively. These results illustrated that most catchments (77 of 92 catchments)  
351 experienced a significant increase trend in the average ACWSC during the

352 transformation from the non-drought period to the prolonged drought period, indicating  
353 a mainstream trend of increased ACWSC during the latter period.

354 The spatial distribution of the 92 catchments that satisfied the criteria of NSE  
355 performance and resultant robustness is presented in **Fig. 5**. Obvious convergence was  
356 found in the spatial distribution of the catchments with different change forms in the  
357 amplitude of the periodic change and the average variation level of the two periods. For  
358 instance, catchments with non-significant change in  $\delta$  were mainly concentrated in the  
359 middle part of the south region of Australia. The reason for this phenomenon may be  
360 the similar physical features and climatic characteristics of adjacent catchments, which  
361 may result in the relatively consistent change direction of catchments in a region.

362 **Fig.6** illustrates the statistical results of the change of amplitude  $\alpha$  and mean value  
363  $\delta$  between two periods (before and after the change point) in all catchments in south-  
364 eastern Australia. **Figs.6(a) and 6(b)** show the absolute and relative change percentage  
365 of amplitude  $\alpha$  between two periods, indicating that the absolute differences in the  
366 amplitude between two periods, i.e.,  $|\alpha_2 - \alpha_1|$  are concentrated within the interval of  
367  $[0, 75]$  for 80.4% of the catchments while the relative changes  $(\alpha_2 - \alpha_1) / \alpha_1$  are mostly  
368 concentrated within the interval of  $[0, 400\%]$  for 69.6% of the catchments. The fitting  
369 curves in **Figs.6(a) and 6(b)**, which were based on the kernel smoother method (Yandell,  
370 1996), had significant positive biases, indicating that much more catchments  
371 experienced an increased tendency in the variation range of periodic changes of the  
372 ACWSC during the drought period. **Figs.6 (c) and 6(d)** show the absolute and relative

373 change percentage of the mean value  $\delta$ , respectively, indicating that the absolute  
374 change of the mean value, i.e.,  $|\delta_2 - \delta_1|$ , are concentrated within the interval of [50, 150]  
375 for 75% of the catchments while the relative change, i.e.,  $(\delta_2 - \delta_1) / \delta_1$ , are mostly  
376 concentrated within the interval of [0, 50%] for 65.2% of the catchments. Similarly, the  
377 fitting curves in **Figs.6(c) and 6(d)** had remarkable positive biases as well, indicating  
378 that much more catchments experienced an increased tendency in the mean value of the  
379 ACWSC after the change point.

380 Among the catchments with significant variation in  $\theta_t$ , two types of typical  
381 catchments were taken as examples to present the specific changes of the ACWSC  
382 (shown in **Fig.7**). In catchment #222206, both  $\alpha_2$  and  $\delta_2$  increased significantly after  
383 the change point compared with  $\alpha_1$  and  $\delta_1$ . Based on the posterior probability of each  
384 possible change point, it was found that the change probability of the ACWSC was the  
385 greatest on 2002/12/27. Changes in  $\theta_t$  indicate that the ACWSC of catchment #222206  
386 tends to increase after the change point. In catchment #421042, the amplitude  $\alpha_2$   
387 decreases significantly while the mean value  $\delta_2$  increases significantly after the  
388 change point. The time corresponding to the change point was 2001/7/30, which refers  
389 to the moment when  $\theta_t$  changes. Therefore, the above results of the two example  
390 catchments suggest that the ACWSC of various catchments may experience different  
391 magnitudes of change under a sustained reduction in rainfall. In addition, a time lag  
392 phenomenon clearly occurred between the onset of the meteorological drought and the  
393 change in  $\theta_t$ .

## 394 **4.2 Response time of catchments with significant change in the** 395 **ACWSC**

396 As mentioned in Section 3.4, the response time refers to the time interval between the  
397 occurrence of the meteorological drought and the change point of the ACWSC. The  
398 magnitude distribution of response time in the 92 catchments that satisfied the basic  
399 criteria of NSE performance and robustness of results was manifested in **Fig.8**, which  
400 indicates that the response time in nearly one-third of the catchments (27/92) fell within  
401 the range of 800-1000 days, followed by the response time of 17 catchments fell within  
402 the range of 600-800 days. Furthermore, as shown in **Table 6**, the average and median  
403 response times of the catchments with significant changes in  $\delta$  are 660.7 days and  
404 750.6 days, respectively. Since no significantly decreased variation in  $\delta$  was found, the  
405 catchments with significant changes in  $\delta$  after the change point all realized a  
406 significantly increased trend. In the catchments with a significant increase in amplitude  
407  $\alpha$ , the average and median estimates of the response time are 660.4 and 750.6 days,  
408 respectively; while those of the catchments with a significant decrease in  $\alpha$  are 391.9  
409 and 422 days, respectively. According to the results shown in **Table 6**, a significant  
410 difference was identified in the length of the response time between two sets of  
411 catchments with a significant increase and decrease in amplitude  $\alpha$ . However, it is not  
412 clear whether the difference between the groups of catchments with significant  
413 increase/decrease change of the amplitude  $\alpha$  is real or just sampling fluctuations.

## 414 **4.3 Factors for shifts in the ACWSC**

415 To provide a better understanding of the response of the variation pattern of the  
416 ACWSC to the prolonged meteorological drought and the variation characteristics  
417 under asymptotic climate change, we investigated whether the change in the ACWSC  
418 (especially in the amplitude  $\alpha$  and mean value  $\delta$ ) was associated with particular  
419 catchment features and/or climate inputs, i.e., are variation in the ACWSC more likely  
420 to occur in the catchments with certain characteristics? Thus, 9 multiple catchment  
421 features and 24 climate variables that may drive the shifts in the variation of the  
422 amplitude  $\alpha$  and mean value  $\delta$  were analyzed in this part.

### 423 **4.3.1 Difference analysis of factors**

#### 424 **4.3.1.1 Difference between groups of catchments with significant and** 425 **non-significant change in $\alpha$**

426 To explore the potential differences in catchment properties and climate inputs  
427 between catchments with different variation patterns, the 92 selected catchments were  
428 divided into two groups (namely  $g_{\alpha}(S)$  (catchments with significant change in  $\alpha$ )  
429 and the  $g_{\alpha}(NS)$  group (catchments with non-significant change in  $\alpha$ )) according to  
430 the significance level of the variation in amplitude  $\alpha$  between the periods before and  
431 after the change point. As illustrated in Table 5,  $g_{\alpha}(S)$  and  $g_{\alpha}(NS)$  groups included  
432 87 and 5 catchments, respectively. 94.6% (87/92) of studied catchments experienced a  
433 significant shift in amplitude  $\alpha$  which indicated that the long-term drought in these

434 catchments resulted in a remarkable change in the variation range of the ACWSC. The  
435 left two columns in each sub-figure of **Fig.9** referred to the statistical features of  
436 catchments within the  $g_{\alpha}(S)$  and  $g_{\alpha}(NS)$  groups. There was a significant  
437 difference in the mean and median estimate of catchment area between these two groups,  
438 with their difference ratio reaching 21.2% and 25.1%, respectively, i.e., the  $g_{\alpha}(NS)$   
439 group indicated a notably larger catchment area than the  $g_{\alpha}(S)$  group. However, no  
440 other features (mentioned in Table 1) showed similarly significant variation between  
441  $g_{\alpha}(S)$  and  $g_{\alpha}(NS)$  groups. Among the adopted 9 catchment features, the results  
442 indicated the difference in the catchment area may be one of the most important factors  
443 for influencing the variation degree of the amplitude  $\alpha$  of the ACWSC. However, due  
444 to the limited number of catchments in the  $g_{\alpha}(NS)$  group (only 5.4% of the adopted  
445 92 catchments), it is still not clear whether the statistical values of this group were real  
446 or just sampling fluctuation.

447 The right two columns in **Fig.9** referred to catchment subsets with a significant  
448 increase pattern in amplitude  $\alpha$  after the change point, namely the  $s_{\alpha}(IS)$  and the  
449  $s_{\alpha}(DS)$  subsets, which denoted the catchment aggregation that experienced  
450 significantly increased and decreased changes after the change point, respectively. It  
451 should be noted that the two subsets were extracted from the  $g_{\alpha}(S)$  group. Most  
452 catchments (95.4% of catchments) experienced a significantly increased change in the  
453 amplitude  $\alpha$  of the ACWSC after the change point, while only 4.6% (4 in 87  
454 catchments) of catchments went through a significantly decreased change after the

455 change point. The increased variation range of the ACWSC that occurred during the  
456 prolonged drought led to a higher fluctuation range of the ACWSC and more intense  
457 variation in runoff generation rate. Thus, the significantly increased pattern in  
458 amplitude  $\alpha$  and more intense variation in runoff generation rate were the mainstream  
459 change direction in the studied catchment dataset.

460 Significant differences have been found in both the mean and median estimate of  
461 features of catchment area and mean elevation between the  $s_\alpha (IS)$  and the  $s_\alpha (DS)$   
462 subsets (see right two columns in **Fig.9**), with the difference ratio reaching 46.7% and  
463 58.5%, respectively. The  $s_\alpha (DS)$  subset had a significantly larger catchment area  
464 than the  $s_\alpha (IS)$  subset. Meanwhile, there was a significant difference in the median  
465 estimate of the  $K_s$  of subsoil between the two subsets, with the difference ratio reaching  
466 27.7%, however, it was non-significant in the mean estimate of the  $K_s$  of subsoil. Due  
467 to the limited number of catchments within the  $s_\alpha (DS)$  subset (only included 4  
468 catchments), it was inadequate to judge whether it was popular findings or just the  
469 uniqueness of the sample.

470 Overall, it was likely that catchments with small areas, low elevations, small slope  
471 ranges, large forest coverage, and high AWHC of soil may change more significantly  
472 in amplitude  $\alpha$  after the interference of the meteorological drought. Generally, small  
473 areas of large forest cover will require considerable (partitioning of) soil water storage.  
474 After experiencing persistent meteorological drought, the pressure on water resources  
475 in the catchment increased and tree cover was lost in large quantities due to withering.



476 Canopy retention and uptake by the forest is an important part of ACWSC, and the  
477 dieback of trees in the forest may result in a significant change in ACWSC (Adams et  
478 al., 2012). Therefore, these catchments are more vulnerable under prolonged drought  
479 due to competition for moisture uptake than catchments with low forest cover and large  
480 areas.

#### 481 **4.3.1.2 Difference between groups of catchments with significant and** 482 **non-significant change in $\delta$**

483 Similarly, we also analyzed the potential relationship between the change in the mean  
484 value  $\delta$  of the ACWSC and the catchment features/climate characteristics. According  
485 to the significance level of the change in mean value  $\delta$ , the 92 catchments were also  
486 segmented into two groups, denoted as  $g_{\delta}(S)$  (catchments with significant change  
487 in  $\delta$ ) and the  $g_{\delta}(NS)$  groups (catchments with non-significant change in  $\delta$ ).

488 As illustrated in **Table 5** and **Fig.10**, 77 in 92 catchments were found to experience  
489 a significantly increased change in the mean value  $\delta$  after the change point, while no  
490 catchment went through a significantly decreased pattern after the change point. The  
491 non-significant change in the mean value  $\delta$  occurred in 15 studied catchments. The  
492 significant increase in the mean value  $\delta$  indicated the increased mean ACWSC after  
493 the change point due to the long-term meteorological drought, resulting the even less  
494 runoff (on average) than the historical relationship suggested. In other words, the low  
495 runoff caused by the reduced rainfall was expected as the previous rainfall-runoff  
496 relationship showed, the increase in the ACWSC may imply an even lower runoff

497 generation rate than expected.

498 The two left columns in each sub-figure of **Fig.10** presented the comparison of  
499 catchment features between  $g_{\delta}(S)$  and  $g_{\delta}(NS)$  groups. There was a significant  
500 difference in the mean (median) estimate of the catchment area, AWHC of the subsoil,  
501 Ks of the subsoil, mean slope and slope range between these two groups, with their  
502 difference ratio reaching 50.3% (33.8%), 34.2% (54.4%), 20.6% (57.1%), 38.8%  
503 (91.1%) and 24.4% (37.4%) respectively. In the other words, the  $g_{\delta}(S)$  group had a  
504 notably smaller catchment area, Ks of the subsoil, mean slope and slope range, and  
505 larger AWHC of the subsoil than the  $g_{\delta}(NS)$  group. Meanwhile, there was a  
506 significant difference in the median estimate of the Ks of topsoil between the two  
507 groups, with the difference ratio reaching 29.6%, however, it was non-significant in the  
508 mean estimate of the Ks of topsoil.

### 509 **4.3.2 Association analysis of factors**

510 **Fig.11** presented the Pearson correlation between the change of amplitude  $\alpha$  of  $\theta_1$   
511 with 9 catchment features and 24 climate variables that were listed in **Table 4**. A  
512 positive association has been identified between the absolute change of amplitude  $\alpha$   
513 and two catchment features (i.e., mean elevation and Ks of subsoil), while negative  
514 relationship between the former and other catchment features (see **Fig.11(a)**). Similarly,  
515 the relative change of amplitude  $\alpha$  was positively associated with only one catchment  
516 feature, i.e., the AWHC of the topsoil (see **Fig.11(b)**). However, no strong correlation  
517 was found between the change of amplitude  $\alpha$  (including both absolute and relative

518 changes) and both catchment features. **Fig.11(c) and (d)** illustrated the possible  
519 correlations between the changes (absolute and relative changes) in the amplitude  $\alpha$  of  
520 the ACWSC and 24 climate variables. Generally, a weak positive correlation was found  
521 between the absolute change of amplitude  $\alpha$  and all climate variables, with the highest  
522 Correlation Coefficient (CC) reaching 0.203 that occurred with the B6 feature (i.e., Cv  
523 of monthly runoff). Similarly, there was no strong correlation between the relative  
524 change of amplitude  $\alpha$  and all climate variables (see **Fig.11(d)**), with the highest CC  
525 only reaching 0.19 that occurred with B17 feature (i.e., the mean annual potential  
526 evapotranspiration). Since no strong correlation was found between the variation in the  
527 amplitude  $\alpha$  and a single factor, we speculated that the potential change of the variation  
528 range of the ACWSC after the change point was the result of the combination of various  
529 catchment properties and climate characteristics.

530 **Fig.12** illustrates the Pearson correlation between the changes (absolute change  
531 and relative change) of the mean value  $\delta$  of the ACWSC and catchment features  
532 between the periods before and after the change point. The absolute change of the mean  
533 value  $\delta$  was negatively correlated with both catchment features (see **Fig. 12(a)**), with  
534 the highest CC reaching -0.362 that occurred with the Ks of topsoil, subsequently  
535 followed by the AWHC of the subsoil (CC=-0.341), the Ks of subsoil (CC=-0.267), and  
536 the forest percentage (CC=-0.242). Similar to **Fig. 12(a)**, the relative change of the  
537 mean value  $\delta$  was negatively correlated with most of catchment features (**Fig. 12(b)**),  
538 except for A3 (slope range) and A8 (AWHC of topsoil), with the largest CC reaching -

539 0.362 that occurred with the  $K_s$  of topsoil, followed by AWHC of the subsoil (CC=-  
540 0.341), and forest coverage (CC=-0.242). It is obvious that the soil and forest-related  
541 features had the largest relationship with the relative change of the mean value  $\delta$   
542 among both catchment features. The potential reasons may lie that the water holding  
543 capacities of various soil types were different due to the dissimilarity of void and  
544 adhesion in different soil types, which directly affected the ability of the catchment to  
545 absorb and store water, thereby influencing the magnitude of the ACWSC of the  
546 catchment (Leblanc et al., 2009). Furthermore, the coverage of various forest  
547 percentages would affect the water holding capacity and water assumption ability  
548 (Fohrer et al., 2005), resulting in potential changes in the ACWSC. **Figs.12(c) and 12(d)**  
549 illustrate the association between the changes (absolute and relative change) of the  
550 mean value  $\delta$  and 24 climate variables before and after the change point. As **Figs.12(c)**  
551 indicates: the absolute change of the mean value  $\delta$  had positive correlations with B19  
552 (Annual aridity index, CC=0.421), followed by B9 (mean summer precipitation,  
553 CC=0.306), while it had negative correlations with B8 and B21. **Fig.12 (d)** shows that  
554 the relative change of the mean value  $\delta$  had the largest negative correlation with B24  
555 (Annual base flow ratio, CC=-0.279), followed by B20 (Mean annual runoff index,  
556 CC=-0.215). No correlation (CC< 0.2) has been found in the relative change of the  
557 mean value  $\delta$  with other climate variables.

558 In total,  $g_\alpha(S)$  and  $g_\delta(S)$  groups had a significantly smaller catchment area  
559 than those of the  $g_\alpha(NS)$  and  $g_\delta(NS)$  groups, indicating the reduced possibility

560 that the ACWSC would change significantly (including changes in both amplitude  $\alpha$   
561 and mean value  $\delta$  ) along with the increased catchment area. Furthermore, the  
562 catchments with a smaller hydraulic conductivity of the soil may be more prone to change  
563 in statistical significance to experience a significant variation on the average level of  
564 the ACWSC during a prolonged meteorological drought.

### 565 **4.3.3 Trend analysis within the significantly changed group**

566 As our findings in **Table 5**, most of the studied catchments experienced a  
567 significantly increased variation after the change point, the  $s_{\alpha} (IS)$  and  $s_{\delta} (IS)$   
568 subsets of catchments were further used as typical samples for the trend analysis  
569 between the variation in the ACWSC and certain characteristics. According to the  
570 results in sections 4.3.1 and 4.3.2, four catchment properties, i.e., catchment area, mean  
571 elevation, forest coverage, and soil characteristics, were adopted for the trend analysis.  
572 As illustrated in **Fig.13**, the absolute changes in  $\alpha$  and  $\delta$  both show an increasing  
573 trend with the increase in catchment area, the catchment group with the mean elevation  
574 within the interval of [300, 600] had the largest absolute change in both the amplitude  
575  $\alpha$  and mean value  $\delta$  among all groups with different elevation interval, implying the  
576 potentially most suitable elevation range for the occurrence of the variation of ACWSC.  
577 Furthermore, the decreased variation of the estimated value of  $\alpha$  and  $\delta$  has been  
578 identified along with the increase in the forest coverage of catchments. In addition,  
579 **Fig.13** indicated that the changes in  $\alpha$  and  $\delta$  were both negatively associated with the  
580 increase in forest coverage percentage of the catchment, implying the positive

581 contribution of high forest coverage to the potential change in the ACWSC during the  
582 meteorological drought. A similar relationship was observed in changes of  $\delta$  with the  
583 AWHC subsoil.

#### 584 **4.4 Factors for the response time of catchments**

585 The Pearson correlation coefficient between the response time with both  
586 catchment features and climate variables was presented in **Fig.14**. Positive correlations  
587 were identified between the response time with A6 (AWHC of the topsoil, CC=0.249)  
588 and A2 (mean elevation, CC=0.239). While a negative correlation was found between  
589 the response time and A5 (forest coverage, CC=-0.225). The potential reasons for this  
590 finding may lie that the larger ACWSC indicated a higher ability of the soil to retain  
591 water and make it more sufficiently available for plant use, thus resulting in an  
592 increased response time in the catchment (Lawes et al., 2009; Leenaars et al., 2018).  
593 Meanwhile, the increased catchment elevation may promote changes in forest  
594 architecture (i.e., decreases in tree stature and stem diameter, trends in stem  
595 deformation, hard, thick, and smaller leaves) and enhance the dominant position of  
596 plants with less water assumption (Lenoir et al., 2008; Oke and Thompson., 2015), and  
597 thus relatively enlarge the response time. In addition, the persistent decline of the  
598 groundwater level and storage has been observed in catchments of South-eastern  
599 Australia (Leblanc et al., 2009), resulting in the gradual reduction of the interactions  
600 between the surface water and groundwater (Van et al., 2013). Thus, the increased forest  
601 coverage of the catchment may result in larger water demand for the ecosystem (Adams

602 et al., 2012), and thus caused a shorter response time of the ACWSC to the  
603 meteorological drought.

604 As for the relationship between the response time and the climate variables  
605 mentioned in **Table 4**, the absolute variations of many climate variables (i.e., B1-B4,  
606 B9, B13, B17) had negative correlations with the response time (**Fig.14(b)**), with their  
607 correlation coefficient between 0.20 and 0.31. The highest CC in **Fig.14(b)** was 0.31  
608 which reached with B2 (mean daily potential evapotranspiration). As shown in  
609 **Fig.14(c)**, the response time was negatively correlated with the absolute change of B2  
610 (mean daily potential evapotranspiration), B3 (mean  $T_{max}$ ), and B13 (mean summer  
611 runoff), with the CC were -0.313, -0.263, and -0.27, respectively. It also should be noted  
612 that only a weak association has been identified between the response time and these  
613 climate variables. In addition, no positive correlation ( $CC > 0.2$ ) has been identified  
614 between the response time with the absolute and relative changes of both climate  
615 variables.

616 Similarly, the potential connections between the response time and several  
617 catchment properties were further analyzed in the significantly changed subsets. As  
618 shown in **Fig.15**, negative associations have been found between the length of response  
619 time with the size of the catchment area and forest coverage. Furthermore, the  
620 catchment group with the mean elevation within the interval of [300, 600] had the  
621 smallest response time within all range groups of catchments.

## 622 **5. Discussions**

### 623 **5.1 Possible reasons for different changes in the ACWSC**

624 The results showed that most catchments were identified to have an increasing trend in  
625 both the amplitude  $\alpha$  and the mean value  $\delta$  of the ACWSC after a prolonged  
626 meteorological drought. According to our findings, soil type and forest coverage are  
627 the variables the most related to the ACWSC. The soil water holding capacities of  
628 various soil types were different due to the dissimilarity of void and adhesion in  
629 different soil types, which directly affects the ability of the catchment to absorb/store  
630 water, thereby affecting the ACWSC of the catchment. Saft et al. (2015) showed that  
631 the annual rainfall-runoff relationships of many catchments changed in southeastern  
632 Australia during the millennium drought (1997-2009). The prolonged meteorological  
633 drought led to the continuous decrease of the groundwater level as well as a significant  
634 change in soil properties. Leblanc's study for southeastern Australia showed that only  
635 two years after the 2001 drought, soil moisture and surface water storage lost 80 and  
636 12 km<sup>3</sup>, respectively, and the rapid drying up reached near-steady low levels (Leblanc  
637 et al., 2009). Years of drought led to an almost complete drying up of surface water  
638 resources, and the hydrological drought continued even after rainfall resumed. In  
639 addition, the soil types in the study area include silt loam, loam, silt, sand, sandy loam,  
640 clay and loamy sand, among which silt loam accounts for more than 45% of the total  
641 study area (Pan et al., 2020). Moreover, the silt loam possessed a strong field capacity  
642 and large adhesion property. The silt loam may maintain the original soil structure state



643 even if the soil pore space increases due to the declined groundwater level, which may  
644 partly explain the increase in the ACWSC of the catchments.

645 Furthermore, the variation of forest coverage and composition would affect the  
646 water holding capacity and water assumption ability, resulting in potential changes in  
647 the ACWSC. Previous studies (Fensham et al., 2009; Allen et al., 2010) showed that  
648 the increased frequency, duration of drought, and heat stress associated with climate  
649 change are strong factors contributing to changes in vegetation dynamics that may  
650 fundamentally alter forest composition and structure in many areas. Drought-induced  
651 vegetation dieback was more likely to occur in regions with relatively high densities of  
652 local woody cover. Adams et al. (2012) combined the extensive literature on the  
653 ecohydrological effects of tree harvesting with existing studies to propose a new and  
654 relevant hypothesis. For most forests, evapotranspiration would be dramatically  
655 reduced after the significant dieback of the tree cover due to drought. According to Pan  
656 et al. (2020), the main land use types throughout the study area are evergreen broadleaf  
657 forest, grassland, woodland, and cropland. As the evergreen broadleaf forest and  
658 woodland occupied most of the study region, the notable loss of tree cover caused by  
659 the prolonged meteorological drought may dramatically reduce the evapotranspiration  
660 in catchments. Catchments with large coverage of evergreen broadleaf forest processed  
661 the large water demand per unit area (Adams et al., 2012). For comparison, the water  
662 consumption of catchments with other land use types (grassland and farmland) was less,  
663 and their drought resistance ability was relatively stronger. It can be hypothesized that

664 in catchments with large coverage of vegetation, the occurrence of the prolonged  
665 drought may intensify the competition for water demand between different varieties of  
666 vegetation, promoting the survival of the vegetation types with less water consumption  
667 but with higher water adoption ability. Therefore, the catchments with high forest cover  
668 may lead to an increase in the ACWSC.

## 669 **5.2 The limitations of the hydrological model**

670 The GR4J model was used to address the response of the ACWSC to the prolonged  
671 meteorological drought. The model processes a relatively simple structure with  
672 relatively low requirements for input data, and it has been widely used in the rainfall-  
673 runoff simulation for small and medium-sized catchments (Dhemi et al., 2010; Demirel  
674 et al., 2013; Sezen et al., 2019; Kunnath et al., 2019). However, the GR4J model is  
675 implemented subject to restrictions and limitations due to the inadequate description of  
676 the runoff generation and flow confluence processes in large catchments (e.g., larger  
677 than 10,000 km<sup>2</sup>). Conceptual models usually consider the entire catchment to be one  
678 entity, then use empirical functional relationships or conceptual simulations to describe  
679 the runoff generation and flow confluence processes, and consequently adopt certain  
680 parameters with physical meanings to characterize the inhomogeneity of the spatial  
681 distribution of catchment characteristics. It has been argued that conceptual lumped  
682 rainfall-runoff models are far from being able to tackle the challenging problem of  
683 assessing the impacts of land use or forest variation. The GR4J model lacks a physical  
684 foundation but seems to best detect changes in a basin behavior (Perrin et al., 2003).

685 According to Westra et al. (2014),  $\theta_1$  is the most sensitive parameter in the GR4J  
686 model and therefore was used to represent the ACWSC in this study. The sine function  
687 was used to reflect the periodic change of the ACWSC. Further studies are necessary  
688 to explore the impacts of different forms of functions on the identification and  
689 simulation of the periodic variation of the ACWSC.

## 690 **6. Conclusions**

691 This study focused on the response of the ACWSC to the long-term meteorological  
692 drought and asymptotic climate change systematically based on the hydrological  
693 simulation method. Firstly, the time-varying parameter (the most sensitive model  
694 parameter in the adopted GR4J model) was derived to reflect the ACWSC  
695 periodic/abrupt variations in drought and non-drought periods. Secondly, the change  
696 points and varying patterns of the ACWSC during the transformation from non-drought  
697 to drought periods were analyzed based on the Bayesian change point analysis with  
698 multiple evaluation criteria. Finally, a variety of catchment features and climate  
699 characteristics were used to explore the possible relationship between these variables  
700 and the temporal variation characteristics of the ACWSC. Catchments that suffered  
701 from the prolonged meteorological drought in southeast Australia were selected as the  
702 case study. The main conclusions were summarized as follows.

703 (1) The increase of ACWSC amplitude change was observed in 83/92 catchments  
704 during the prolonged drought period, and significant shifts in the mean value of the  
705 ACWSC were detected in 77/92 catchments.

706 (2) The average response time of the ACWSC for all 92 catchments with  
707 significant changes was 641.3 days. Specifically, the response time in 27 and 17  
708 catchments fell within the ranges of 800-1000 days and 600-800 days, respectively.

709 (3) The ACWSC changed significantly in the catchments with small areas, low  
710 elevations, small slope ranges, large forest coverage, and high soil water holding  
711 capacities.

712 In this study, the response characteristics of the ACWSC to the prolonged  
713 meteorological drought in southeastern Australia were analyzed. It was found that the  
714 catchment response time and mode are greatly different. However, only the correlations  
715 between the changes of parameter  $\theta_l$ , response time, and single-factor of catchment  
716 features and climate variables were considered in this study. Subsequent studies could  
717 be conducted by combining data from multiple sources to carry out multi-factor  
718 regression analysis. Nevertheless, this study could enhance our understanding of the  
719 variations in catchment property under climate change.

## 720 **Acknowledgments**

721 This study was supported by the National Natural Science Foundation of China (Grant  
722 No. U20A20317) and the National Key Research and Development Program of China  
723 (2021YFC3200303). The numerical calculations were done on the supercomputing  
724 system in the Supercomputing Center of Wuhan University. The authors would like to  
725 thank the editor and anonymous reviewers for their comments, which helped improve  
726 the quality of the paper.

727 **Author contributions**

728 All the authors helped to conceive and design the analysis. Jing Tian and Zhengke Pan  
729 performed the analysis and wrote the paper. Shenglian Guo, Jun Wang, Jiabo Yin and  
730 Yanlai Zhou contributed to the writing of the paper and made comments.

731 **Compliance with ethical standards**

732 **Conflict of interest:** The authors declare that they have no conflict of interest.

733 **References**

- 734 Abbaspour, K. C., Yang, J., Maximov, I., Siber, R., Bogner, K., Mieleitner, J., Zobrist, J., and Srinivasan,  
735 R.: Modelling hydrology and water quality in the pre-alpine/alpine Thur watershed using SWAT, *J.*  
736 *Hydrol.*, 333, 413-430, 10.1016/j.jhydrol.2006.09.014, 2007.
- 737 Adams, H. D., Luce, C. H., Breshears, D. D., Allen, C. D., Weiler, M., Hale, V. C., Smith, A. M. S., and  
738 Huxman, T. E.: Ecohydrological consequences of drought- and infestation- triggered tree die-off:  
739 insights and hypotheses, *Ecohydrology*, 5, 145-159, 10.1002/ecc.233, 2012.
- 740 Ajami, N. K., Duan, Q. Y., and Sorooshian, S.: An integrated hydrologic Bayesian multimodel  
741 combination framework: Confronting input, parameter, and model structural uncertainty in  
742 hydrologic prediction, *Water Resour. Res.*, 43, 10.1029/2005wr004745, 2007.
- 743 Allen, C. D., Macalady, A. K., Chenchouni, H., Bachelet, D., McDowell, N., Vennetier, M., Kitzberger,  
744 T., Rigling, A., Breshears, D. D., Hogg, E. H., Gonzalez, P., Fensham, R., Zhang, Z., Castro, J.,  
745 Demidova, N., Lim, J. H., Allard, G., Running, S. W., Semerci, A., and Cobb, N.: A global overview  
746 of drought and heat-induced tree mortality reveals emerging climate change risks for forests, *For.*  
747 *Ecol. Manage.*, 259, 660-684, 10.1016/j.foreco.2009.09.001, 2010.
- 748 Bayat, B., Nasserli, M., and Zahraie, B.: Identification of long-term annual pattern of meteorological  
749 drought based on spatiotemporal methods: evaluation of different geostatistical approaches, *Nat.*  
750 *Hazards*, 76, 515-541, 10.1007/s11069-014-1499-3, 2015.
- 751 Brigode, P., Oudin, L., and Perrin, C.: Hydrological model parameter instability: A source of additional  
752 uncertainty in estimating the hydrological impacts of climate change?, *J. Hydrol.*, 476, 410-425,  
753 10.1016/j.jhydrol.2012.11.012, 2013.
- 754 Cahill, N., Rahmstorf, S., and Parnell, A. C.: Change points of global temperature, *Environ. Res. Lett.*,  
755 10, 10.1088/1748-9326/10/8/084002, 2015.
- 756 Carlin, B. P., Gelfand, A. E., and Smith, A. F. M.: Hierarchical bayesian-analysis of changepoint  
757 problems, *J. R. Stat. Soc. C-Appl.*, 41, 389-405, 10.2307/2347570, 1992.
- 758 Carrer, G. E., Klaus, J., and Pfister, L.: Assessing the Catchment Storage Function Through a Dual-  
759 Storage Concept, *Water Resour. Res.*, 55, 476-494, 10.1029/2018wr022856, 2019.
- 760 Changnon, D., and Gensini, V. A.: Changing Spatiotemporal Patterns of 5-and 10-Day Illinois Heavy

761       Precipitation Amounts, 1900-2018, *J. Appl. Meteorol. Clim.*, 58, 1523-1533, 10.1175/jamc-d-18-  
762       0335.1, 2019.

763       Chawla, I., and Mujumdar, P. P.: Isolating the impacts of land use and climate change on streamflow,  
764       *Hydrol. Earth Syst. Sc.*, 19, 3633-3651, 10.5194/hess-19-3633-2015, 2015.

765       Chen, Q. H., Chen, H., Wang, J. X., Zhao, Y., Chen, J., and Xu, C. Y.: Impacts of Climate Change and  
766       Land-Use Change on Hydrological Extremes in the Jinsha River Basin, *Water*, 11,  
767       10.3390/w11071398, 2019.

768       Coron, L., Andreassian, V., Perrin, C., Lerat, J., Vaze, J., Bourqui, M., and Hendrickx, F.: Crash testing  
769       hydrological models in contrasted climate conditions: An experiment on 216 Australian catchments,  
770       *Water Resour. Res.*, 48, 10.1029/2011wr011721, 2012.

771       Costa, M. H., Botta, A., and Cardille, J. A.: Effects of large-scale changes in land cover on the discharge  
772       of the Tocantins River, Southeastern Amazonia, *J. Hydrol.*, 283, 206-217, 10.1016/s0022-  
773       1694(03)00267-1, 2003.

774       Das, S., Das, J., and Umamahesh, N. V.: Identification of future meteorological drought hotspots over  
775       Indian region: A study based on NEX-GDDP data, *Int. J. Climatol.*, 41, 5644-5662,  
776       10.1002/joc.7145, 2021.

777       Demirel, M. C., Booij, M. J., and Hoekstra, A. Y.: Effect of different uncertainty sources on the skill of  
778       10 day ensemble low flow forecasts for two hydrological models, *Water Resour. Res.*, 49, 4035-  
779       4053, 10.1002/wrcr.20294, 2013.

780       Deng, C., Liu, P., Guo, S. L., Li, Z. J., and Wang, D. B.: Identification of hydrological model parameter  
781       variation using ensemble Kalman filter, *Hydrol. Earth Syst. Sc.*, 20, 4949-4961, 10.5194/hess-20-  
782       4949-2016, 2016.

783       Deng, C., Liu, P., Wang, D. B., and Wang, W. G.: Temporal variation and scaling of parameters for a  
784       monthly hydrologic model, *J. Hydrol.*, 558, 290-300, 10.1016/j.jhydrol.2018.01.049, 2018.

785       Fensham, R. J., Fairfax, R. J., and Ward, D. P.: Drought-induced tree death in savanna, *Global Change*  
786       *Biol.*, 15, 380-387, 10.1111/j.1365-2486.2008.01718.x, 2009.

787       Fohrer, N., Haverkamp, S., and Frede, H. G.: Assessment of the effects of land use patterns on hydrologic  
788       landscape functions: development of sustainable land use concepts for low mountain range areas,  
789       *Hydrol. Process.*, 19(3), 659-672, 10.1002/hyp.5623, 2005.

790       Gao, H., Hrachowitz, M., Schymanski, S. J., Fenicia, F., Sriwongsitanon, N., and Savenije, H. H. G.:  
791       Climate controls how ecosystems size the root zone storage capacity at catchment scale, *Geophys.*  
792       *Res. Lett.*, 41, 7916-7923, 10.1002/2014gl061668, 2014.

793       Huang, S. Z., Li, P., Huang, Q., Leng, G. Y., Hou, B. B., and Ma, L.: The propagation from meteorological  
794       to hydrological drought and its potential influence factors, *J. Hydrol.*, 547, 184-195,  
795       10.1016/j.jhydrol.2017.01.041, 2017.

796       Hughes, J. D., Petrone, K. C., and Silberstein, R. P.: Drought, groundwater storage and stream flow  
797       decline in southwestern Australia, *Geophys. Res. Lett.*, 39, 10.1029/2011gl050797, 2012.

798       Hunt, B. G.: Multi-annual dry episodes in Australian climatic variability, *Int. J. Climatol.*, 29, 1715-1730,  
799       10.1002/joc.1820, 2009.

800       Jeremiah, E., Marshall, L., Sisson, S. A., and Sharma, A.: Specifying a hierarchical mixture of experts  
801       for hydrologic modeling: Gating function variable selection, *Water Resour. Res.*, 49, 2926-2939,  
802       10.1002/wrcr.20150, 2013.

803 Jung, I. W., Moradkhani, H., and Chang, H.: Uncertainty assessment of climate change impacts for  
804 hydrologically distinct river basins, *J. Hydrol.*, 466, 73-87, 10.1016/j.jhydrol.2012.08.002, 2012.

805 Kumar, A., Panda, K. C., Nafil, M., and Sharma, G.: Identification of meteorological drought  
806 characteristics and drought year based on rainfall departure analysis, *J. Appl. Sci. Technol.*, 51-59,  
807 2020.

808 Kundu, S., Khare, D., and Mondal, A.: Individual and combined impacts of future climate and land use  
809 changes on the water balance, *Ecol. Eng.*, 105, 42-57, 10.1016/j.ecoleng.2017.04.061, 2017.

810 Kunnath-Poovakka, A., and Eldho, T. I.: A comparative study of conceptual rainfall-runoff models GR4J,  
811 AWBM and Sacramento at catchments in the upper Godavari river basin, India, *J. Earth Syst. Sci.*,  
812 128, 10.1007/s12040-018-1055-8, 2019.

813 Kusangaya, S., Warburton, M. L., van Garderen, E. A., and Jewitt, G. P. W.: Impacts of climate change  
814 on water resources in southern Africa: A review, *Phys. Chem. Earth*, 67-69, 47-54,  
815 10.1016/j.pce.2013.09.014, 2014.

816 Laurène, J. E., Bouaziz, Aalbers, E. E., Weerts, A.H., Hegnauer, M., and Hrachowitz, M.: The importance  
817 of ecosystem adaptation on hydrological model predictions in response to climate change, *Hydrol.*  
818 *Earth Syst. Sc.*, 2021.

819 Lawes, R. A., Oliver, Y. M., Robertson, M. J.: Integrating the effects of climate and plant available soil  
820 water holding capacity on wheat yield, *Field Crop. Res.*, 113(3), 297-305, 10.1016/j.fcr.2009.06.008,  
821 2009.

822 Le Moine, N., Andreassian, V., and Mathevet, T.: Confronting surface- and groundwater balances on the  
823 La Rochefoucauld-Touvre karstic system (Charente, France), *Water Resour. Res.*, 44,  
824 10.1029/2007wr005984, 2008.

825 Leblanc, M. J., Tregoning, P., Ramillien, G., Tweed, S. O., and Fakes, A.: Basin-scale, integrated  
826 observations of the early 21st century multiyear drought in southeast Australia, *Water Resour. Res.*,  
827 45, 10.1029/2008wr007333, 2009.

828 Leenaars, J. G. B., Claessens, L., Heuvelink, G. B. M., et al. Mapping rootable depth and root zone plant-  
829 available water holding capacity of the soil of sub-Saharan Africa, *Geoderma*, 324, 18-36,  
830 10.13140/RG.2.1.3950.9209, 2018.

831 Lenoir, J., Gégout, J. C., Marquet, P. A., de Ruffray, P., and Brisse, H.: A significant upward shift in plant  
832 species optimum elevation during the 20th century, *Science*, 320(5884), 1768-1771,  
833 10.1016/j.idairyj.2006.12.007, 2008.

834 Lin, B. Q., Chen, X. W., Yao, H. X., Chen, Y., Liu, M. B., Gao, L., and James, A.: Analyses of landuse  
835 change impacts on catchment runoff using different time indicators based on SWAT model, *Ecol.*  
836 *Indicators*, 58, 55-63, 10.1016/j.ecolind.2015.05.031, 2015.

837 McNamara, J. P., Tetzlaff, D., Bishop, K., Soulsby, C., Seyfried, M., Peters, N. E., Aulenbach, B. T., and  
838 Hooper, R.: Storage as a metric of catchment comparison, *Hydrol. Process.*, 25, 3364-3371,  
839 10.1002/hyp.8113, 2011.

840 Melsen, L., Teuling, A., Torfs, P., Zappa, M., Mizukami, N., Clark, M., and Uijlenhoet, R.:  
841 Representation of spatial and temporal variability in large-domain hydrological models: case study  
842 for a mesoscale pre-Alpine basin, *Hydrol. Earth Syst. Sc.*, 20, 2207-2226, 10.5194/hess-20-2207-  
843 2016, 2016.

844 Nepal, S., Chen, J., Penton, D. J., Neumann, L. E., Zheng, H. X., and Wahid, S.: Spatial GR4J

845 conceptualization of the Tamor glaciated alpine catchment in Eastern Nepal: evaluation of GR4JSG  
846 against streamflow and MODIS snow extent, *Hydrol. Process.*, 31, 51-68, 10.1002/hyp.10962, 2017.

847 Nicholls, N.: The changing nature of Australian droughts, *Clim. Change*, 63, 323-336,  
848 10.1023/B:CLIM.0000018515.46344.6d, 2004.

849 Nijzink, R., Hutton, C., Pechlivanidis, I., Capell, R., Arheimer, B., Freer, J., Han, D., Wagener, T.,  
850 McGuire, K., Savenije, H., and Hrachowitz, M.: The evolution of root-zone moisture capacities  
851 after deforestation: a step towards hydrological predictions under change?, *Hydrol. Earth Syst. Sc.*,  
852 20, 4775-4799, 10.5194/hess-20-4775-2016, 2016.

853 Oke, O. A., Thompson, K. A.: Distribution models for mountain plant species: the value of elevation,  
854 *Ecol. Model.*, 301, 72-77, 10.1016/j.ecolmodel.2015.01.019, 2015.

855 Pan, Z. K., Liu, P., Gao, S. D., Cheng, L., Chen, J., and Zhang, X. J.: Reducing the uncertainty of time-  
856 varying hydrological model parameters using spatial coherence within a hierarchical Bayesian  
857 framework, *J. Hydrol.*, 577, 10.1016/j.jhydrol.2019.123927, 2019a.

858 Pan, Z. K., Liu, P., Gao, S. D., Xia, J., Chen, J., and Cheng, L.: Improving hydrological projection  
859 performance under contrasting climatic conditions using spatial coherence through a hierarchical  
860 Bayesian regression framework, *Hydrol. Earth Syst. Sc.*, 23, 3405-3421, 10.5194/hess-23-3405-  
861 2019, 2019b.

862 Pan, Z. K., Liu, P., Xu, C. Y., Cheng, L., Tian, J., Cheng, S. J., and Xie, K.: The influence of a prolonged  
863 meteorological drought on catchment water storage capacity: a hydrological-model perspective,  
864 *Hydrol. Earth Syst. Sc.*, 24, 4369-4387, 10.5194/hess-24-4369-2020, 2020.

865 Patil, S. D., and Stieglitz, M.: Comparing Spatial and temporal transferability of hydrological model  
866 parameters, *J. Hydrol.*, 525, 409-417, 10.1016/j.jhydrol.2015.04.003, 2015.

867 Perrin, C., Michel, C., and Andreassian, V.: Improvement of a parsimonious model for streamflow  
868 simulation, *J. Hydrol.*, 279, 275-289, 10.1016/s0022-1694(03)00225-7, 2003.

869 Potter, N. J., Petheram, C., and Zhang, L.: Sensitivity of streamflow to rainfall and temperature in south-  
870 eastern Australia during the Millennium drought, 19th International Congress on Modelling and  
871 Simulation (MODSIM), Perth, Australia, 2011, WOS:000314989303087, 3636-3642, 2011.

872 Saft, M., Western, A. W., Zhang, L., Peel, M. C., and Potter, N. J.: The influence of multiyear drought on  
873 the annual rainfall-runoff relationship: An Australian perspective, *Water Resour. Res.*, 51, 2444-  
874 2463, 10.1002/2014wr015348, 2015.

875 Saft, M., Peel, M. C., Western, A. W., and Zhang, L.: Predicting shifts in rainfall-runoff partitioning  
876 during multiyear drought: Roles of dry period and catchment characteristics, *Water Resour. Res.*,  
877 52, 9290-9305, 10.1002/2016wr019525, 2016.

878 Sezen, C., and Partal, T.: The utilization of a GR4J model and wavelet-based artificial neural network for  
879 rainfall-runoff modelling, *Water Supply*, 19, 1295-1304, 10.2166/ws.2018.189, 2019.

880 Shen, M. X., Chen, J., Zhuan, M. J., Chen, H., Xu, C. Y., and Xiong, L. H.: Estimating uncertainty and  
881 its temporal variation related to global climate models in quantifying climate change impacts on  
882 hydrology, *J. Hydrol.*, 556, 10-24, 10.1016/j.jhydrol.2017.11.004, 2018.

883 Simonneaux V, H. L., Boulet G, et al.: Modelling runoff in the Rheraya Catchment (High Atlas, Morocco)  
884 using the simple daily model GR4J., Trends over the last decades [C]//13th IWRA World Water  
885 Congress, Montpellier, France., 2008.

886 Singh, C., Wang-Erlandsson, L., Fetzer, I., Rockstrom, J., and van der Ent, R.: Rootzone storage capacity



887 reveals drought coping strategies along rainforest-savanna transitions, *Environ. Res. Lett.*, 15,  
888 10.1088/1748-9326/abc377, 2020.

889 Siriwardena, L., Finlayson, B. L., and McMahon, T. A.: The impact of land use change on catchment  
890 hydrology in large catchments: The Comet River, Central Queensland, Australia, *J. Hydrol.*, 326,  
891 199-214, 10.1016/j.jhydrol.2005.10.030, 2006.

892 Thiemann, M., Trosset, M., Gupta, H., and Sorooshian, S.: Bayesian recursive parameter estimation for  
893 hydrologic models, *Water Resour. Res.*, 37, 2521-2535, Doi 10.1029/2000wr900405, 2001.

894 Tian, J., Guo, S. L., Deng, L. L., Yin, J. B., Pan, Z. K., He, S. K., and Li, Q. X.: Adaptive optimal  
895 allocation of water resources response to future water availability and water demand in the Han  
896 River basin, China, *Sci. Rep.*, 11, 10.1038/s41598-021-86961-1, 2021.

897 Tu, J.: Combined impact of climate and land use changes on streamflow and water quality in eastern  
898 Massachusetts, USA, *J. Hydrol.*, 379, 268-283, 10.1016/j.jhydrol.2009.10.009, 2009.

899 van Dijk, A., Beck, H. E., Crosbie, R. S., de Jeu, R. A. M., Liu, Y. Y., Podger, G. M., Timbal, B., and  
900 Viney, N. R.: The Millennium Drought in southeast Australia (2001-2009): Natural and human  
901 causes and implications for water resources, ecosystems, economy, and society, *Water Resour. Res.*,  
902 49, 1040-1057, 10.1002/wrcr.20123, 2013.

903 Van Lanen, H. A. J., Wanders, N., Tallaksen, L. M., and Van Loon, A. F.: Hydrological drought across  
904 the world: impact of climate and physical catchment structure, *Hydrol. Earth Syst. Sc.*, 17, 1715-  
905 1732, 10.5194/hess-17-1715-2013, 2013.

906 Vrugt, J. A., Gupta, H. V., Bouten, W., and Sorooshian, S.: A Shuffled Complex Evolution Metropolis  
907 algorithm for optimization and uncertainty assessment of hydrologic model parameters, *Water*  
908 *Resour. Res.*, 39, 10.1029/2002wr001642, 2003.

909 Westra, S., Thyer, M., Leonard, M., Kavetski, D., and Lambert, M.: A strategy for diagnosing and  
910 interpreting hydrological model nonstationarity, *Water Resour. Res.*, 50, 5090-5113,  
911 10.1002/2013wr014719, 2014.

912 Yandell, B. S.: Kernel Smoothing, *Technometrics*, 38, 75-76, 1996.

913 Zeng, L., Xiong, L. H., Liu, D. D., Chen, J., and Kim, J. S.: Improving Parameter Transferability of GR4J  
914 Model under Changing Environments Considering Nonstationarity, *Water*, 11, 10.3390/w11102029,  
915 2019.

916 Zhang, Y. Q., Viney, N., Frost, A., Oke, A., Brooks, M., Chen, Y., and Campbell, N.: Collation of  
917 Australian modeller's streamflow dataset for 780 unregulated Australian catchments, CSIRO: Water for  
918 a healthy country national research flagship, 115 pp, 2013.

919

920 **Tables**

921 **Table 1.** Description of the dataset adopted in this study.

922

Data type	Description	Data source
Meteorological data	Daily precipitation, potential evapotranspiration	
Runoff data	Daily runoff data from hydrological stations	Australian Water Resources Assessment system
Catchment features	Catchment area, elevation, slope, forest coverage percentage, AWHC of the soil, $K_s$ of the soil	

923 **Note:** AWHC denotes the available soil water holding capacity;  $K_s$  refers to the saturated hydraulic  
924 conductivity.

925

926

927 **Table 2.** Summary of the characteristics of the 145 catchments that had the prolonged  
928 meteorological drought, including the mean, median, minimum, and  
929 maximum estimates of 9 catchment features.

930

Number	Catchment features	Mean	Median	Minimum	Maximum
A1	Area (km <sup>2</sup> )	711.17	363.0	54.0	6818.0
A2	Mean elevation (m)	542.57	468.0	47.0	1351.0
A3	Slope range (°)	22.18	22.6	2.1	49.9
A4	Mean slope (°)	5.49	5.0	0.3	13.6
A5	Forest coverage (%)	55.00	57.0	15.0	92.0
A6	AWHC of the topsoil (mm)	41.26	42.0	22.0	64.0
A7	AWHC of the subsoil (mm)	88.66	87.5	27.0	188.0
A8	K <sub>s</sub> of topsoil (mm/h)	157.52	160.0	31.0	283.0
A9	K <sub>s</sub> of subsoil (mm/h)	62.10	53.0	4.0	216.0

931

932

933  
934  
935

**Table 3.** Ranges of the initial values of GR4J model parameters.

Parameters	Meaning	Unit	Min	Max	
$\alpha_1, \alpha_2$	Amplitude of the sine function	/	-200	200	
$\theta_1$	$\beta_1, \beta_2$	Frequency of the sine function	/	0	1
	$\gamma_1, \gamma_2$	Remainder in the sine function	/	-200	200
	$\delta_1, \delta_2$	Intercept of the sine function	/	-300	300
$\theta_2$	Groundwater exchange coefficient	mm	-5.0	5.0	
$\theta_3$	Capacity of catchment reservoir	mm	1.0	200.0	
$\theta_4$	Unit line confluence time	day	0.1	10.0	

936  
937

938 **Table 4. Category of the** selected variables that may be associated with the changes in  
 939 the ACWSC. The selected variables was divided into two parts, i.e., cathment features  
 940 (9 variables) and climate variables (24 variables).

941

<b>Category</b>	<b>Catchment features</b>	<b>Category</b>	<b>Climate variables</b>
A1	Area (km <sup>2</sup> )	A6	AWHC of the topsoil (mm)
A2	Mean elevation (m)	A7	AWHC of the subsoil (mm)
A3	Slope range (°)	A8	K <sub>s</sub> of topsoil (mm/h)
A4	Mean slope (°)	A9	K <sub>s</sub> of subsoil (mm/h)
A5	Forest coverage (%)		
<b>Category</b>	<b>Climate variables</b>	<b>Category</b>	<b>Climate variables</b>
B1	Mean daily precipitation (mm)	B13	Mean summer runoff(mm)
B2	Mean daily potential evapotranspiration(mm)	B14	Mean autumn runoff(mm)
B3	Mean Daily T <sub>max</sub> (°C)	B15	Mean winter runoff(mm)
B4	Mean Daily T <sub>min</sub> (°C)	B16	Mean annual precipitation (mm)
B5	C <sub>v</sub> of monthly precipitation	B17	Mean annual potential evapotranspiration(mm)
B6	C <sub>v</sub> of monthly runoff	B18	Mean annual runoff(mm)
B7	Mean monthly runoff index	B19	Mean annual aridity ratio
B8	Mean spring precipitation (mm)	B20	Mean annual runoff index
B9	Mean summer precipitation (mm)	B21	C <sub>v</sub> of annual precipitation
B10	Mean autumn precipitation (mm)	B22	C <sub>v</sub> of annual runoff
B11	Mean winter precipitation (mm)	B23	Mean annual base flow (mm)
B12	Mean spring runoff(mm)	B24	Annual base flow ratio

942

943 **Table 5.** Summary of catchments with different change patterns in the amplitude  $\alpha$   
 944 and mean value  $\delta$  in the regression function of the ACWSC due to a prolonged  
 945 meteorological drought.

946

Factors	Magnitude	Change direction	Number of catchments	Percentage	
Amplitude ( $\alpha$ )	Significant change	Increased	83	57.24%	
		Decreased	4	2.76%	
	Non-significant change	Increased	3	2.07%	
		Decreased	2	1.38%	
	Catchments that do not meet the criteria for the maximum performance degradation and result robustness			53	36.55%
	Catchments with a prolonged meteorological drought			145	100%
Mean value ( $\delta$ )	Significant change	Increased	77	53.10%	
		Decreased	0	0	
	Non-significant change	Increased	10	6.90%	
		Decreased	5	3.45%	
	Catchments that do not meet the criteria of the maximum performance degradation and result robustness			53	36.55%
	Catchments with a prolonged meteorological drought			145	100%

947

948

949 **Table 6.** Response times of different groups of catchments with significant increase/  
950 decrease in regression parameters  $\alpha$  and  $\delta$  .

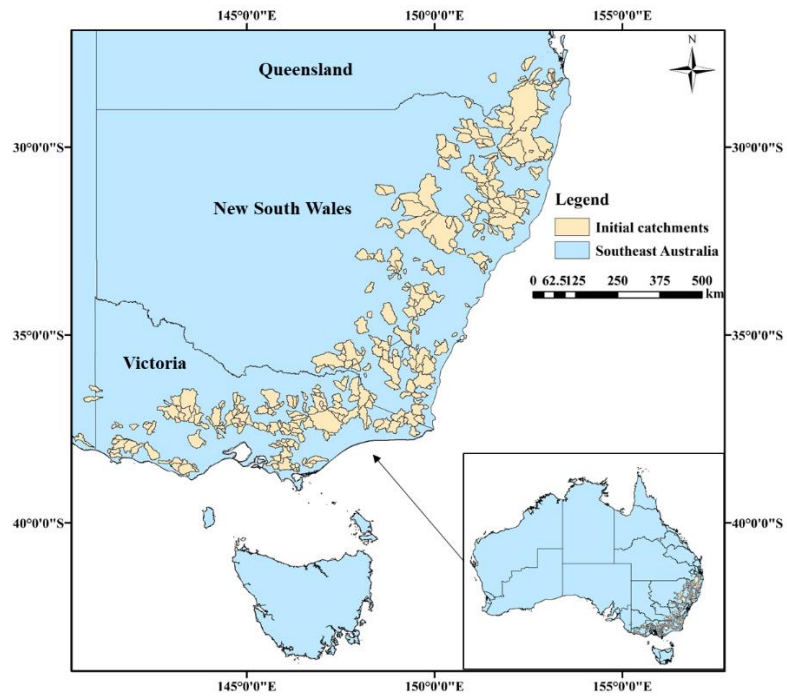
951

Catchment type	Average (day)	Median (day)	Minimum (day)	Maximum (day)
Catchments with significant increase in $\delta$	691.1	781.0	92.2	1082.0
Catchments with significant decrease in $\delta$	/	/	/	/
Catchments with significant increase in $\alpha$	690.8	781.0	92.2	1082.0
Catchments with significant decrease in $\alpha$	422.3	452.4	122.6	661.9

952

953 **Figures**

954

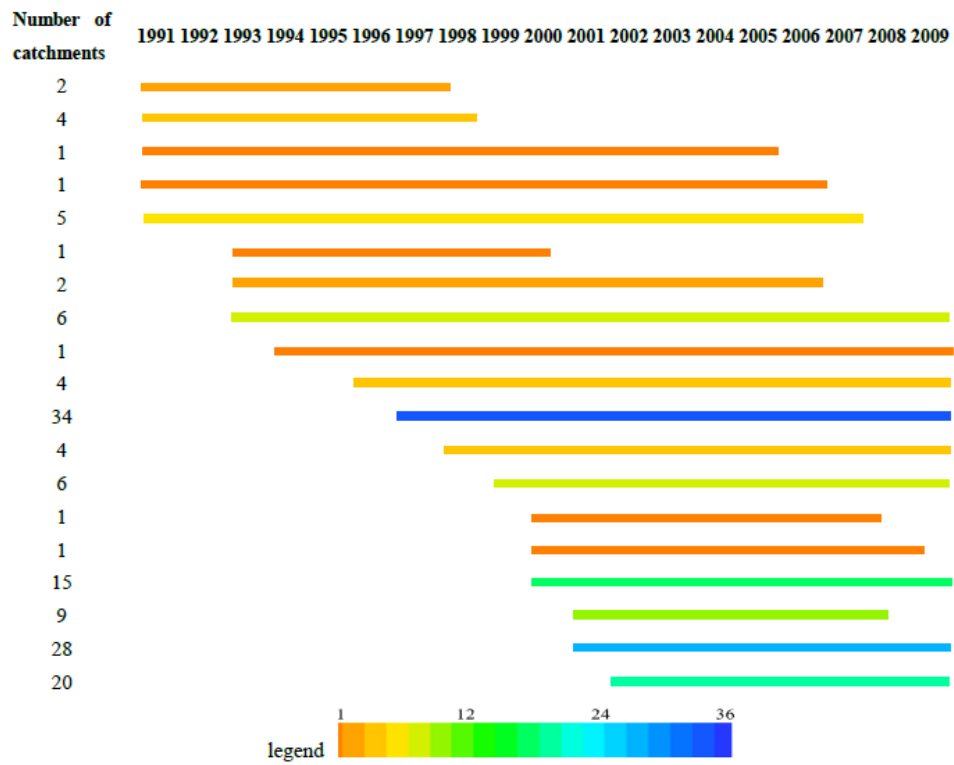


955

956 **Fig.1.** Spatial distribution of the original 398 catchments in south-eastern Australia

957 that were selected from Zhang et al. (2013).

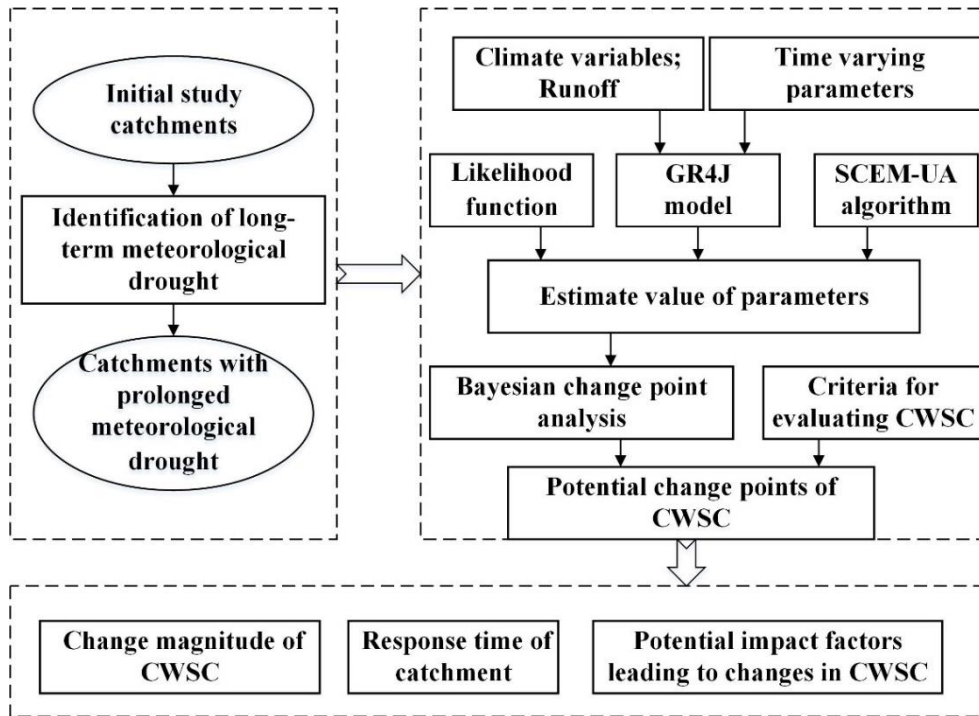




959

960

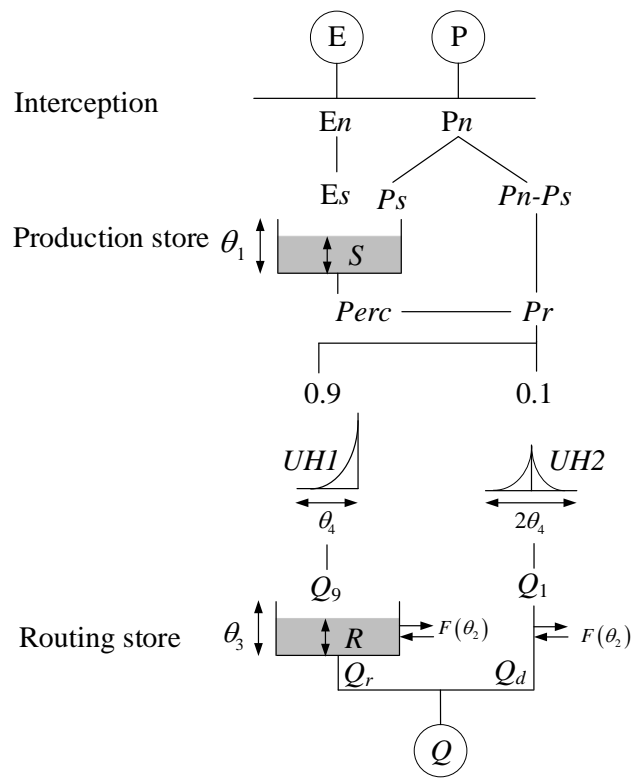
961 **Fig.2.** The drought periods correspond to 145 catchments with prolonged  
 962 meteorological drought in the south-eastern Australia.



963

964

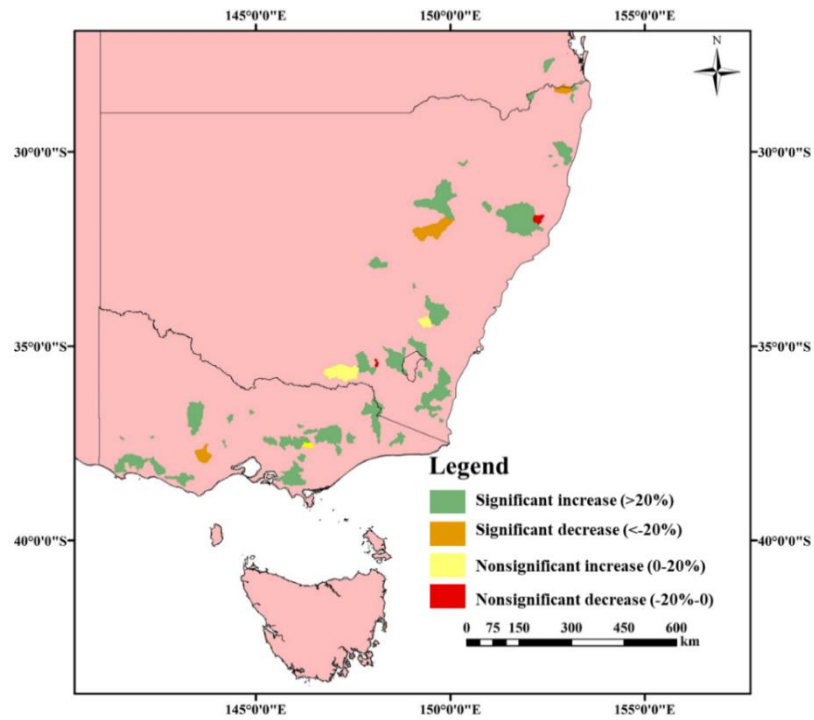
**Fig.3.** Flowchart of the proposed methodology and procedures.



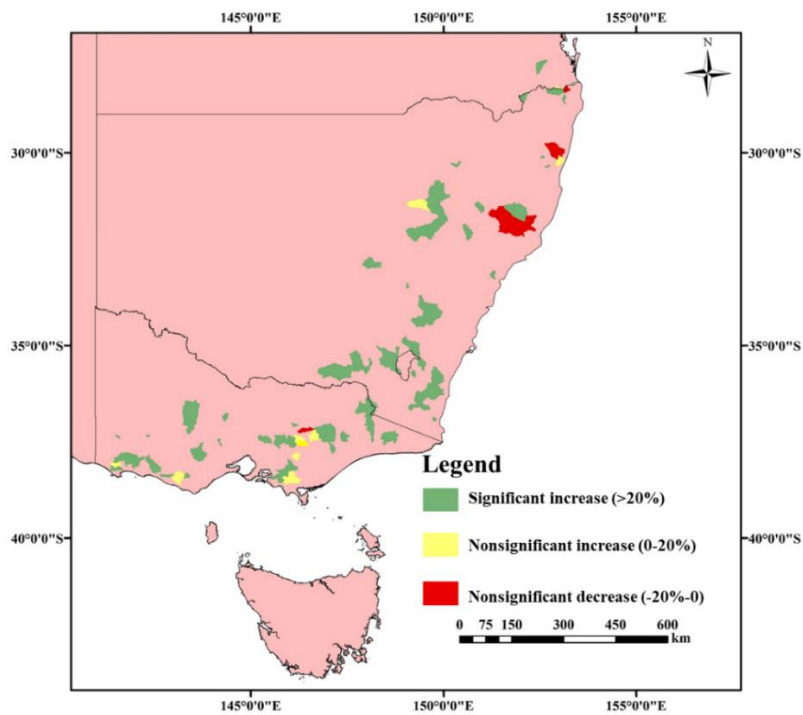
965

966

**Fig.4.** Diagram of the GR4J model proposed by Perrin et al. (2003).



(a) Amplitude  $\alpha$

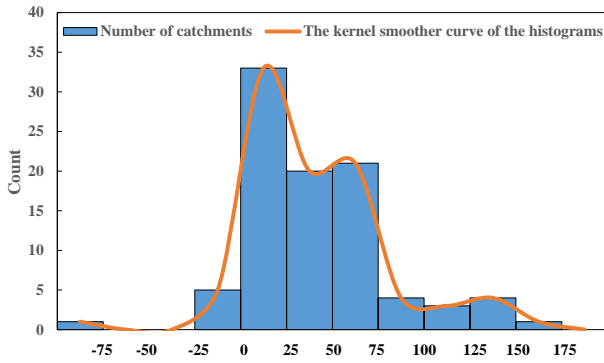


(b) Mean value  $\delta$

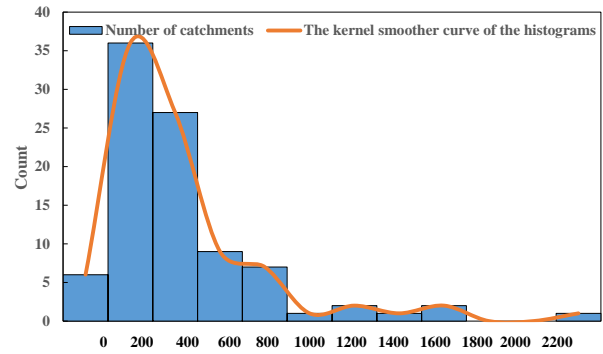
**Fig.5.** Spatial distribution of catchments with different change patterns in the ACWSC after the prolonged drought. Subfigures (a) and (b) illustrate the spatial distribution of catchments with different variation forms in the amplitude  $\alpha$  and mean value  $\delta$  during the drought period, respectively.

967  
968

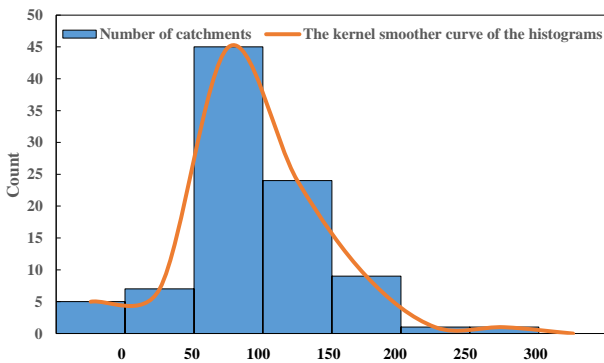
969  
970  
971  
972  
973  
974



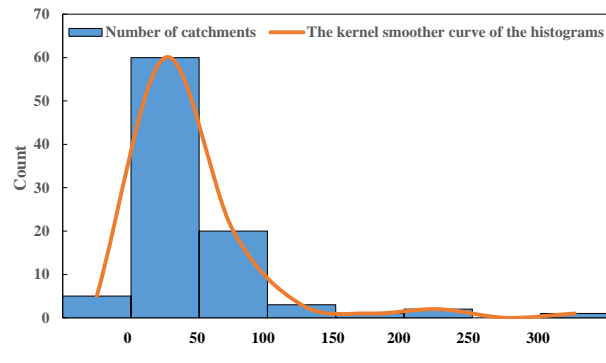
(a) Magnitude of absolute change in estimated parameter  $\alpha$



(b) Magnitude of the relative change percentage in estimated parameter  $\alpha$



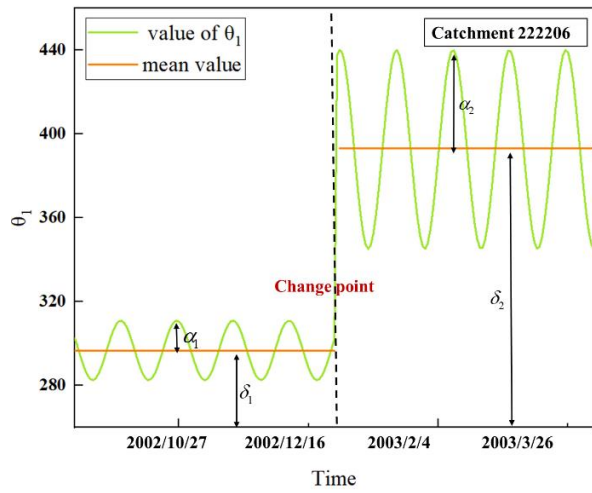
(c) Magnitude of absolute change in estimated parameter  $\delta$



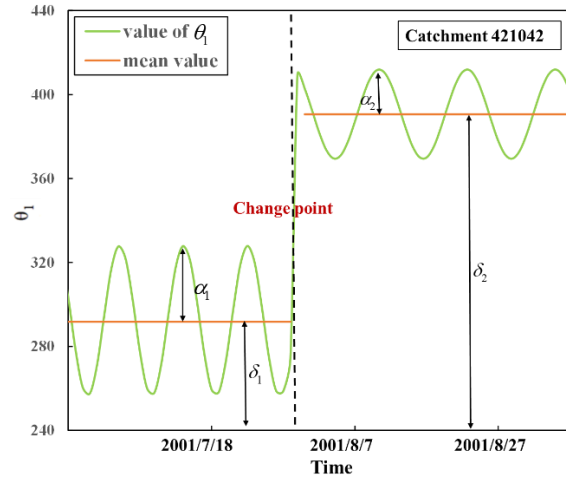
(d) Magnitude of the relative change percentage in estimated parameter  $\delta$

975

976 **Fig.6.** The magnitudes of change in the amplitude and mean value of the ACWSC  
 977 between the periods before and after the change point. Sub-figures (a) and (b) illustrate  
 978 the magnitude of absolute and relative percentage changes in estimated parameter  $\alpha$  ,  
 979 respectively. Sub-figures (c) and (d) refer to magnitude of absolute and relative  
 980 percentage changes in the estimated mean value of parameter  $\delta$  .



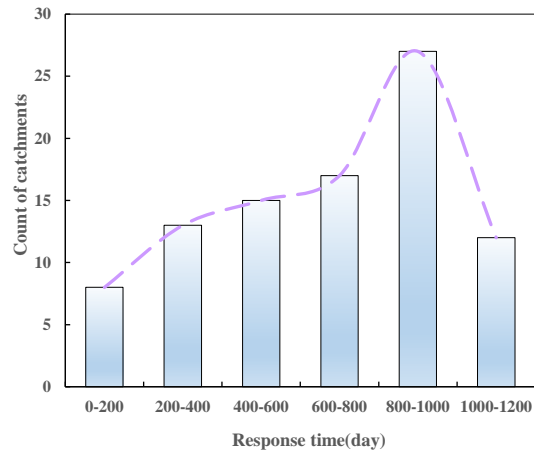
(a) Catchment 222206



(b) Catchment 421042

981

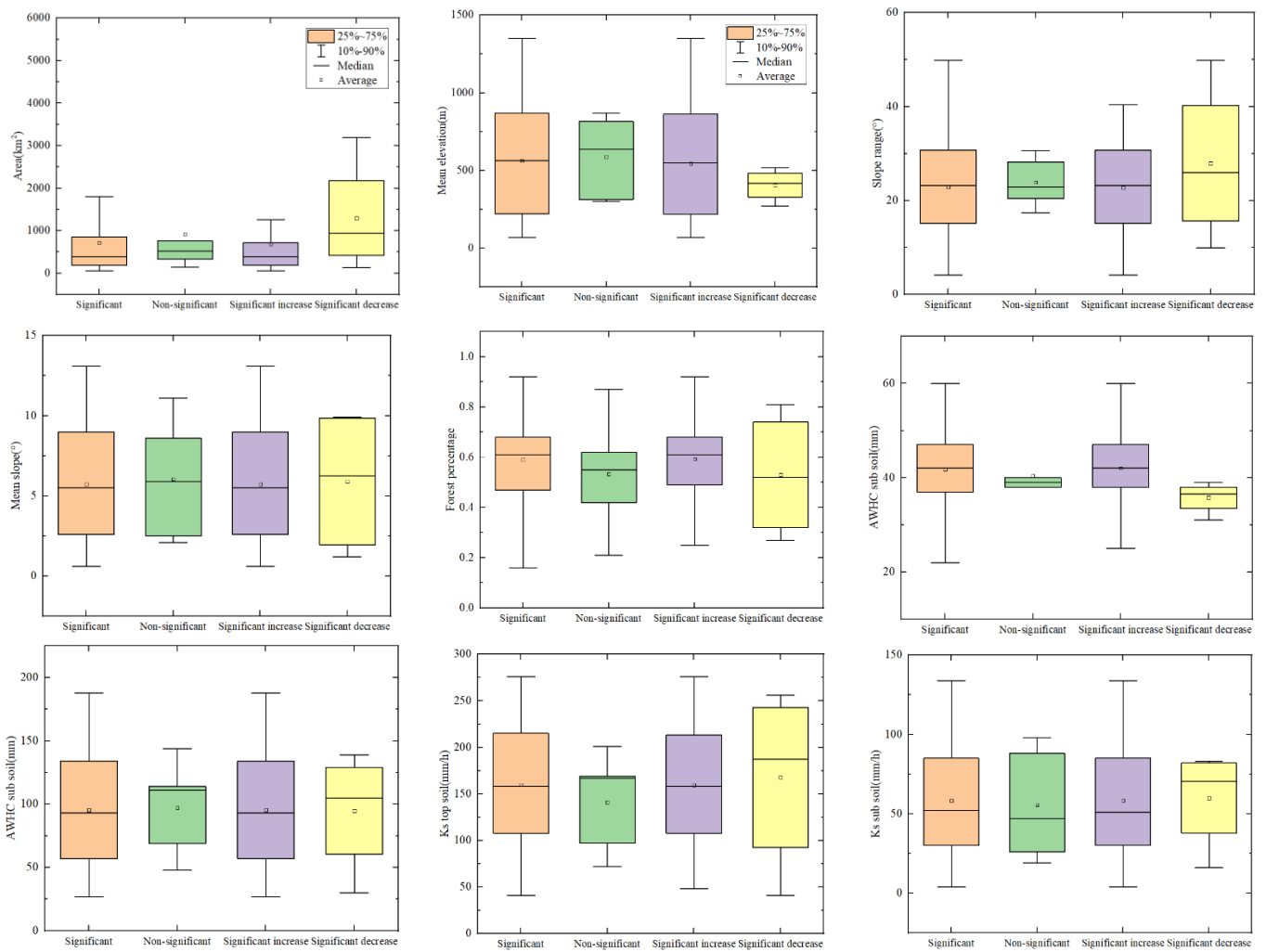
982 **Fig.7.** Time-varying patterns of model parameter  $\theta_l$  in two example catchments (i.e.,  
 983 catchment 222206 and 421042).



984

985 **Fig.8.** Magnitude distribution of the response time in 92 catchments that satisfied the  
986 basic criteria of NSE performance and result robustness.

987



988

989 **Fig.9.** Comparison of physical features between the  $g_{\alpha}(S)$  and  $g_{\alpha}(NS)$  groups and

990  $g_{\alpha}(SI)$  and  $g_{\alpha}(SD)$  subsets for the study catchments. The orange and green boxes (left

991 two columns) denote the physical characteristics of the  $g_{\alpha}(S)$  and  $g_{\alpha}(NS)$  groups

992 which was divided according to the significance level of the variation in the amplitude

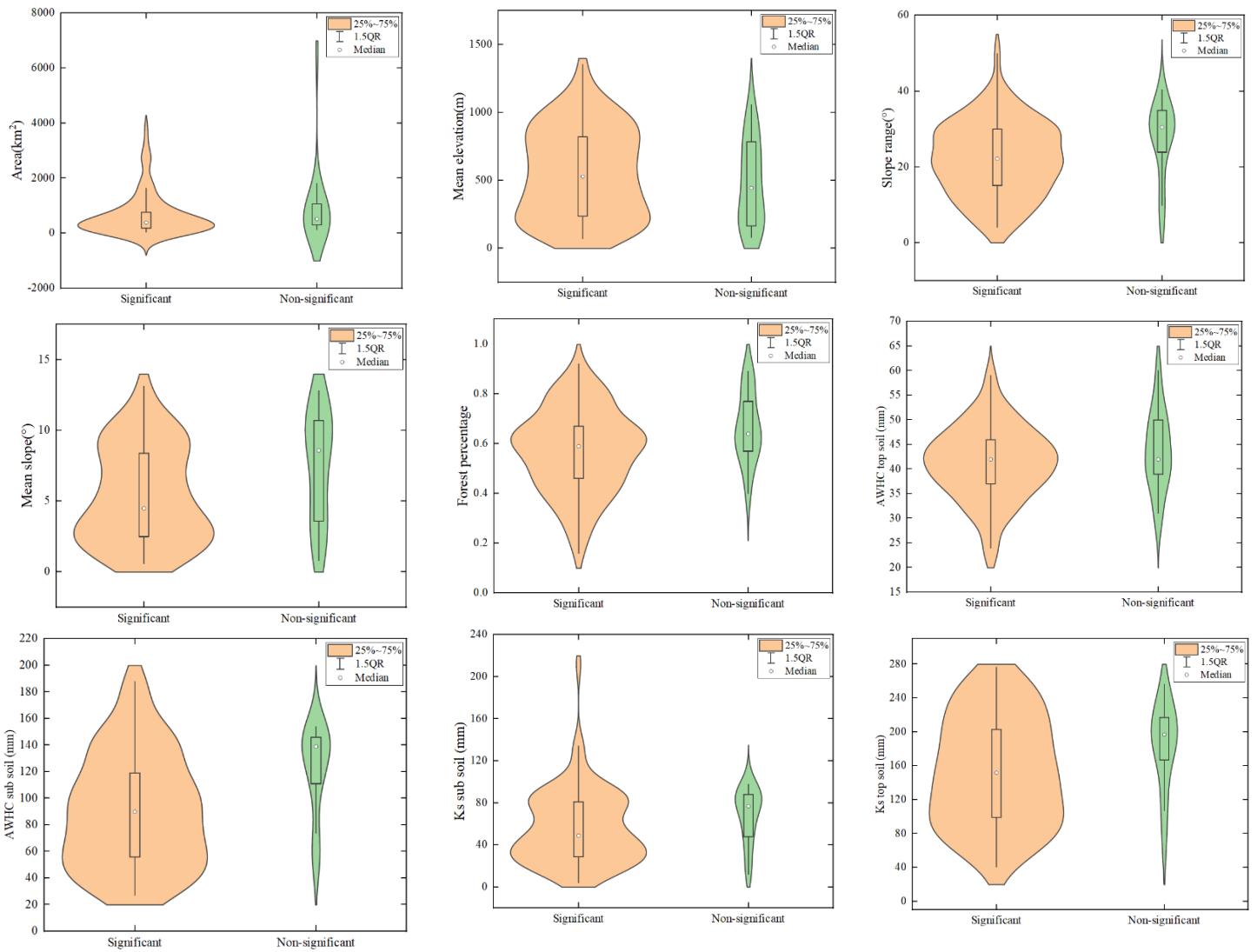
993 after the change point. The purple and yellow columns (right two columns) denote the

994 catchment features of the  $g_{\alpha}(SI)$  and  $g_{\alpha}(SD)$  subsets with significantly increased and

995 decreased change patterns in the amplitude after the change point, respectively.

996

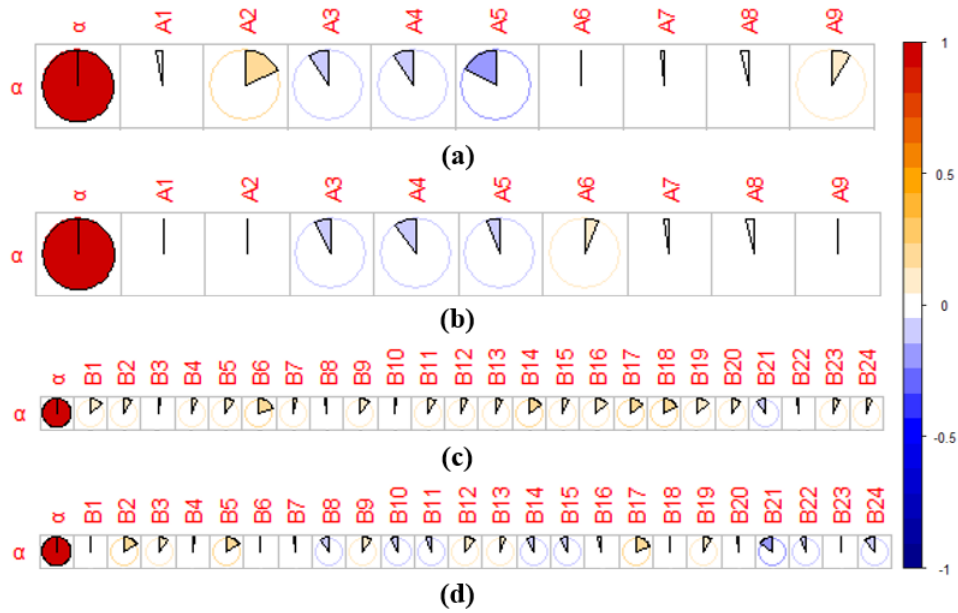




999 **Fig.10.** Comparison of catchment characteristics between the groups of catchments

1000 with significant and non-significant changes in mean value  $\delta$ , i.e.,  $g_\delta(s)$  and

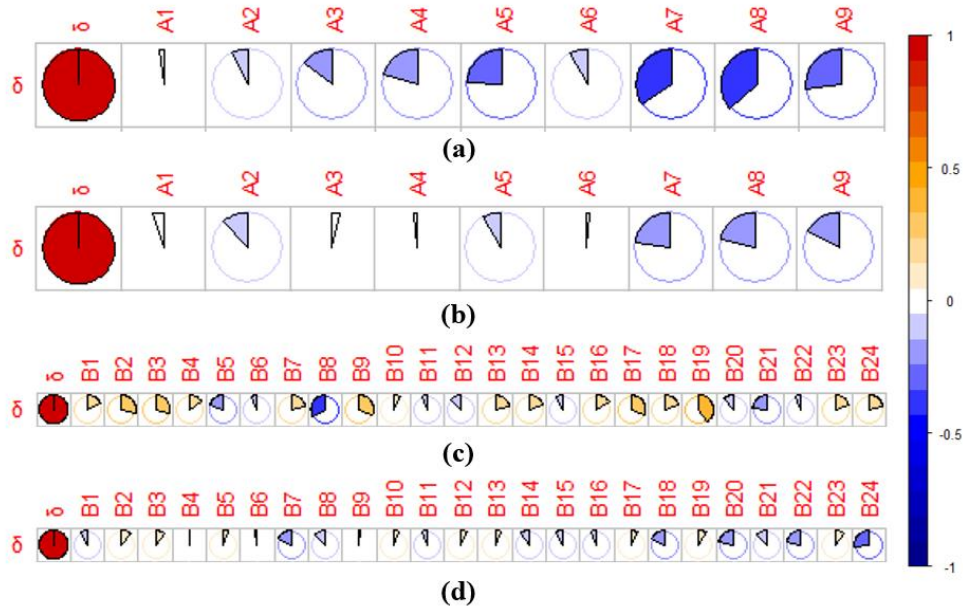
1001 the  $g_\delta(NS)$  groups.



1002

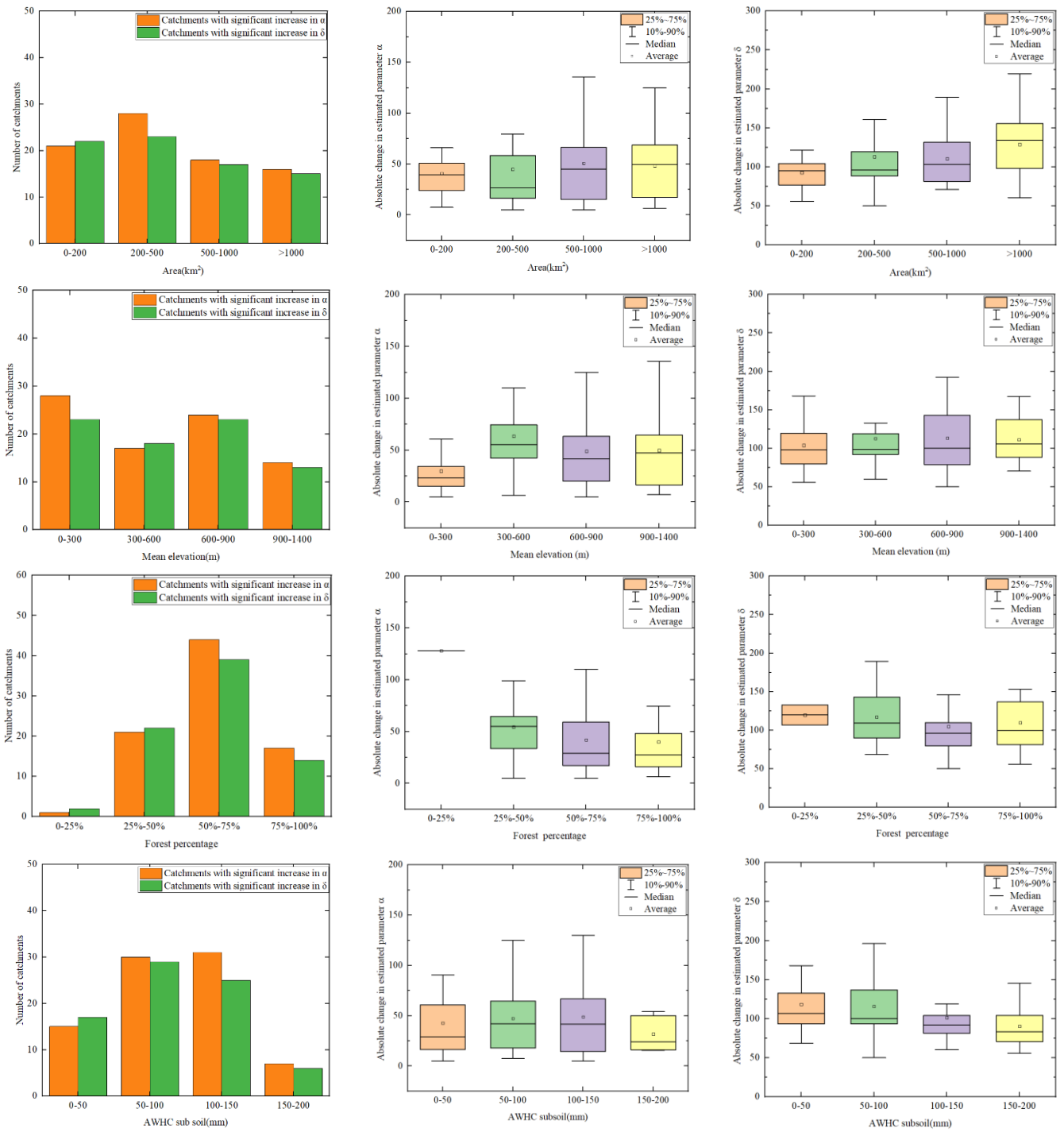
1003 **Fig.11.** The Pearson correlation coefficient between the variation in the amplitude  $\alpha$   
 1004 with multiple catchments features and climate variables. (a) Correlation between the  
 1005 absolute variation of amplitude  $\alpha$  and catchment features; (b) Correlation between the  
 1006 relative variation of amplitude  $\alpha$  and catchment features; (c) Correlation between the  
 1007 absolute variation of amplitude  $\alpha$  and absolute variation of climate variables; (d)  
 1008 Correlation between the relative variation of amplitude  $\alpha$  and relative variation of  
 1009 climate variables.

1010



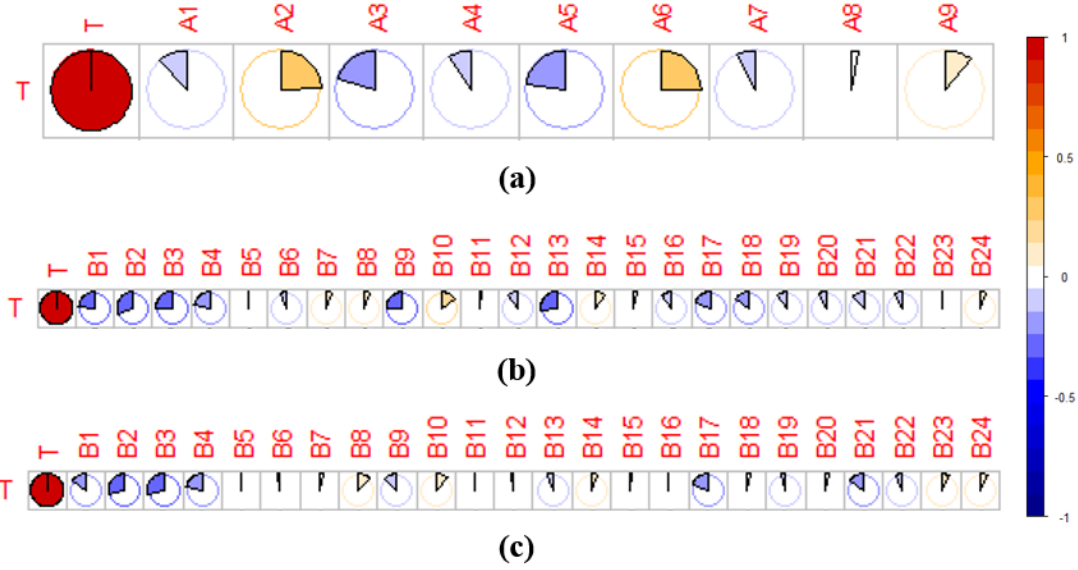
1011

1012 **Fig.12.** The Pearson correlation coefficient between the variation in the mean value  $\delta$   
1013 with multiple catchment features and climate variables. (a) Correlation between the  
1014 absolute variation of mean value  $\delta$  and catchment features; (b) Correlation between  
1015 the relative variation of mean value  $\delta$  and catchment features; (c) Correlation between  
1016 the absolute variation of mean value  $\delta$  and absolute variation of climate variables; (d)  
1017 Correlation between the relative variation of mean value  $\delta$  and relative variation of  
1018 climate variables.



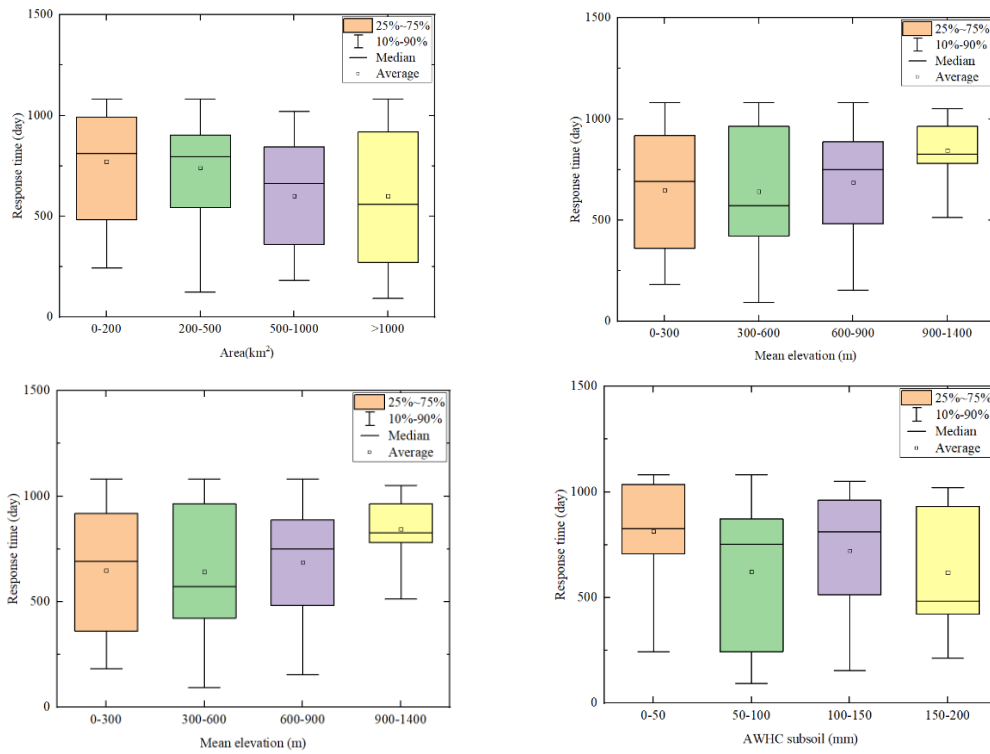
1019 **Fig.13.** Trend analysis between the variation in the ACWSC and catchment properties.

1020



1021

1022 **Fig.14.** The Pearson correlation coefficient between the response time with catchment  
1023 features and variation in climate variables before and after the change point. (a)  
1024 Correlation between the response time and catchment features; (b) Correlation between  
1025 the response time and absolute change of climate variables; (c) Correlation between the  
1026 response time and relative change of climate variables.



1027

1028 **Fig.15.** The potential connections between the response time and catchment properties.